Ocean Sci., 21, 3195–3219, 2025 https://doi.org/10.5194/os-21-3195-2025 © Author(s) 2025. This work is distributed under the Creative Commons Attribution 4.0 License.





Dense shelf water and associated sediment transport in the Cap de Creus Canyon and adjacent shelf under mild winter regimes: insights from the 2021–2022 winter

Marta Arjona-Camas^{1,2}, Xavier Durrieu de Madron², François Bourrin², Helena Fos¹, Anna Sanchez-Vidal¹, and David Amblas¹

¹GRC Geociències Marines, Departament de Dinàmica de la Terra i de l'Oceà, Universitat de Barcelona, Barcelona, Spain ²CEFREM, UMR-5110 CNRS-Université de Perpignan Via Domitia, Perpignan, France

Correspondence: Marta Arjona-Camas (marjona@ub.edu)

Received: 20 March 2025 – Discussion started: 28 March 2025

Revised: 16 October 2025 - Accepted: 22 October 2025 - Published: 27 November 2025

Abstract. Dense shelf water cascading (DSWC) is a key oceanographic process in transferring energy and matter from continental shelves to deep ocean areas. Although intense DSWC (IDSWC) events have received most attention due to their large impacts, mild DSWC (MDSWC) events are the most frequent in the northwestern Mediterranean and are expected to become more common under climate change. However, their dynamics, particularly in the Cap de Creus Canyon, have been less comprehensively described and compared to strong-winter events. This study investigates MDSWC in the Cap de Creus Canyon during the mild winter of 2021-2022, examining shelf-canyon transports of both dense shelf waters and suspended particulate matter (SPM). Observations from the FARDWO-CCC1 multiplatform cruise in March 2022 revealed the presence of cold, dense, and turbid shelf waters, enriched in dissolved oxygen and chlorophyll a, on the continental shelf adjacent to the canyon. These waters cascaded into the canyon head and progressed further into the canyon along its southern flank to \sim 390 m depth. Estimated water and SPM transports during this event were 0.7 Sv and 10⁵ metric tons (t), respectively, at the continental shelf. Within the canyon, transports were 0.3 Sv and 10⁵ metric tons in the upper section, while midcanyon transports were lower $(0.05 \text{ Sy} \text{ and } 10^4, \text{ respectively}),$ indicating that most dense shelf waters likely remained confined to the shelf area and upper canyon. During this event, dense shelf waters were transported $\sim 30 \, \mathrm{km}$ from the shelf into the canyon. Our results show that significant transport of dense shelf waters (260 km³) and suspended sediment can

occur in the Cap de Creus Canyon during MDSWC events under mild winters, also contributing significantly to the formation of Western Intermediate Water (WIW) in the canyon. The Mediterranean Sea Physics reanalysis data indicate that the cascading season lasted from late-January to mid-March 2022, with several shallow cascading pulses throughout this period. Peak transport occurred in mid-March associated with an eastern storm, which likely intensified MDSWC in the canyon. Our study reinforces the idea that dense shelf water transports exhibit marked interannual variability, even under mild winters.

1 Introduction

Continental margins are dynamic transition zones that connect the terrestrial and ocean systems, and play a key role in the transfer and redistribution of particulate material (Nittrouer et al., 2009; Levin and Sibuet, 2012). These regions often receive substantial inputs of sediment, especially from rivers and atmospheric deposition (Blair and Aller, 2012; Liu et al., 2016; Kwon et al., 2021). While much of this material accumulates on the continental shelf, various hydrodynamic processes, such as storm waves, river floods, or ocean currents, can resuspend and transport sediments towards the continental slope and deeper areas of the ocean (Walsh and Nittrouer, 2009; Puig et al., 2014).

One particularly efficient mechanism of shelf-to-slope exchanges is dense shelf water cascading (DSWC). DSWC is

a seasonal oceanographic phenomenon that occurs in marine regions worldwide. DSWC starts when surface waters over the continental shelf become denser than surrounding waters by cooling, evaporation, or sea-ice formation with brine rejection (e.g., Ivanov et al., 2004; Durrieu de Madron et al., 2005; Canals et al., 2006; Amblas and Dowdeswell, 2018; Mahjabin et al., 2019, 2020; Gales et al., 2021). Dense shelf waters then sink, generating near-bottom gravity flows that move downslope, frequently funneled through submarine canyons (Allen and Durrieu de Madron, 2009). This process contributes to the ventilation of the deep ocean, and plays an important role in the global thermohaline circulation. Additionally, it modifies the seabed along its path by eroding and depositing sediments, and facilitates the transfer of energy and matter (including sediment particles, organic carbon, pollutants, and litter) from shallow to deep waters (Canals et al., 2006; Tubau et al., 2013; Puig, 2017; Amblas and Dowdeswell, 2018).

The Gulf of Lion (GoL), located in the northwestern Mediterranean, is a very interesting region to study DSWC and shelf-slope exchanges. This region receives important inputs from riverine discharge and atmospheric deposition, and is subject to intense physical forcing (Durrieu de Madron et al., 2008). Episodic events, such as storms or DSWC, efficiently contribute to the export of shelf waters and sediments towards the open sea and deeper parts of the basin (Millot, 1990; Canals et al., 2006; Palanques et al., 2006, 2008; Ogston et al., 2008). The formation of dense waters in the GoL essentially occurs in winter, triggered by persistent (> 30 consecutive days) northerly and north-westerly winds (locally named Tramontane and Mistral) that induce surface heat loss, evaporation, vertical mixing, and the subsequent densification of shelf waters (Durrieu de Madron et al., 2005, 2008; Canals et al., 2006; Durrieu de Madron et al., 2013). These dense waters sink until reaching their equilibrium depth and propagate along the western coast of the GoL (Fig. 1). The combined effect of the prevailing cyclonic coastal circulation and the narrowing of the continental shelf near the Cap de Creus Peninsula (Fig. 1), concentrates most of this dense water at the southwestern end of the GoL, where it is mainly exported through the Lacaze-Duthiers and Cap de Creus canyons (Ulses et al., 2008b; Palanques et al., 2008). In these canyons, dense waters overspill the shelf edge and cascade down the slope (Béthoux et al., 2002; Durrieu de Madron et al., 2005), contributing to the ventilation of intermediate and deep layers. As they descend, these overflows reshape the seabed by eroding and depositing sediments, and promote the downslope transport of organic matter accumulated on the shelf. Ultimately, DSWC in the GoL has been observed to impact biogeochemical cycles and the functioning of deep-sea ecosystems (Bourrin and Durrieu de Madron, 2006; Bourrin et al., 2008; Heussner et al., 2006; Sanchez-Vidal et al., 2008).

Due to its relative ease of access, the GoL is particularly suitable for investigating DSWC. However, because

of its intermittent nature, DSWC remains difficult to observe directly and its contribution to shelf-slope exchanges is challenging to quantify. Several studies in the GoL have focused on the impact of intense DSWC (IDSWC) events on shelf-slope exchanges. These particularly extreme events were monitored in the winters of 1998-1999 (Heussner et al., 2006), 2004-2005 (Canals et al., 2006; Ogston et al., 2008; Puig et al., 2008), 2005-2006 (Sanchez-Vidal et al., 2008; Pasqual et al., 2010), and 2011-2012 (Durrieu de Madron et al., 2013; Palanques and Puig, 2018), with instrumented mooring lines deployed at ~1000 m depth in Lacaze-Duthiers and Cap de Creus Canyons. One of the most studied IDSWC events occurred in the severe winter of 2004–2005, when over 40 d, more than two thirds (750 km³) of GoL's shelf waters cascaded through the Cap de Creus Canyon (Canals et al., 2006; Ulses et al., 2008b). This event was characterized by cold temperatures (11-12.7 °C), high densities ($\sigma\theta \ge 29.1 \,\mathrm{kg} \,\mathrm{m}^{-3}$), strong down-canyon velocities ($> 0.8 \,\mathrm{m\,s^{-1}}$), and high suspended sediment concentrations (30–40 mg L⁻¹), and transported $\sim 0.6 \times 10^6$ t of organic carbon downcanyon, a mass comparable to the mean annual solid transport of all rivers discharging into the GoL (Canals et al., 2006; Tesi et al., 2010). Although IDSWC events have drawn particular attention due to their significant impacts, mild or shallow DSWC (MDSWC) events are in fact the most frequent since the set of the observational era in the GoL, and they are expected to become more prevalent under climate change (Herrmann et al., 2008; Durrieu de Madron et al., 2023). These events typically occur during mild winters, characterized by quieter atmospheric conditions and lower heat losses (Martín et al., 2013; Rumín-Caparrós et al., 2013; Mikolajczak et al., 2020). During such winters, the cold continental winds that drive dense water formation are weaker and less persistent, typically blowing for fewer than 30 d and rarely exceeding speeds of 10 m s⁻¹. In contrast, easterly and southeasterly winds become unusually more frequent and sustained, sometimes blowing for more than three consecutive days (Ferré et al., 2008). They do not produce a densification of surface waters but lead to an intense cyclonic circulation on the GoL's shelf (Ulses et al., 2008a; Mikolajczak et al., 2020). At the same time, river discharges, particularly from the Rhône River, supply freshwater to the GoL's shelf, further limiting locally the densification of shelf waters (Ulses et al., 2008a). The cyclonic circulation on the shelf can promote the accumulation of light shelf waters $(\sigma\theta \approx 27.78 \,\mathrm{kg}\,\mathrm{m}^{-3})$ along the coast and their subsequent downwelling into the Cap de Creus Canyon, without cascading off-shelf (Martín et al., 2013; Rumín-Caparrós et al., 2013). Under mild winter conditions, shelf waters can continue to gain density on the shelf, reaching $\sigma\theta \approx 28.9$ - 29.1 kg m^{-3} and cascading typically to depths $\sim 400 \text{ m}$ depth into the canyon. This shallow cascading allows dense shelf waters to descent just above the intermediate-water layer, where they contribute to the formation of Western Intermedi-

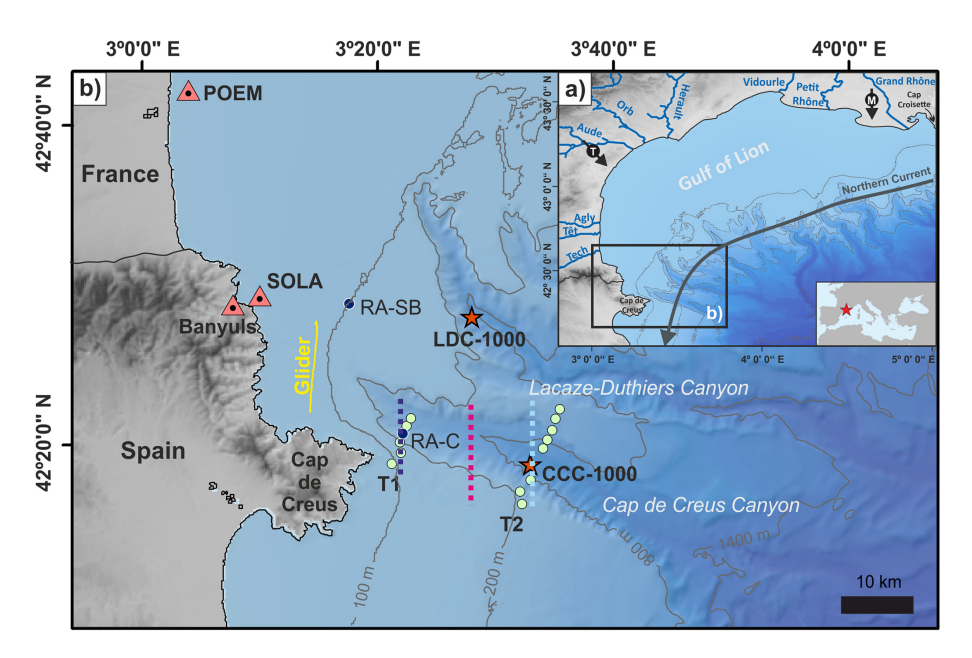


Figure 1. (a) Bathymetric map of the GoL showing the rivers discharging into the gulf and the incised submarine canyons. Black arrows depict Tramontane and Mistral winds. The grey arrow indicates the direction of the Northern Current over the study area. **(b)** Bathymetric map of the southwestern part of the Gulf of Lion showing the location of Lacaze-Duthiers Canyon (LDC) and Cap de Creus Canyon (CCC). Orange triangles indicate the location of buoys (POEM, Banyuls, and SOLA). The location of the re-analysis grid-points at the shelf break (RA-SB) and within the CCC (RA-C) are indicated with dark blue dots. Green dots represent the location of CTD stations carried out during the FARDWO-CCC1 cruise. Red stars mark the location of two instrumented mooring lines deployed at ~ 1000 m depth at the axis of LDC (LDC-1000) and CCC (CCC-1000). The solid yellow line indicates the glider section on the continental shelf adjacent to the CCC. Dashed lines correspond to the virtual transects defined using reanalysis data: dark blue and light blue lines indicate the location of the upper and mid-canyon transects, respectively, used to estimate dense water transport during winter 2021–2022; the fuchsia dashed line marks the central canyon transect used to determine the temporal evolution of cascading events over the past 26 years (1997–2022).

ate Water (WIW) (Dufau-Julliand et al., 2004; Herrmann et al., 2008).

The mechanisms driving MDSWC events during mild winters are relatively well described, but their magnitude and contribution to shelf-to-slope exchanges remain less quantified. Previous studies have provided first-order estimates of dense water transports during MDSWC events. For instance, Ulses et al. (2008a) estimated a total transport of dense shelf waters of 75 km³ in the mild winter of 2003–2004, an order of magnitude smaller than during IDSWC events. More recently, modeling studies have expanded our understanding on the interannual variability of dense water transports under different atmospheric scenarios, and emphasized the role of mild winters in driving MDSWC events in the GoL (Mikolajczak et al., 2020). Nonetheless, most existing studies have relied on numerical simulations or time series from fixed mooring stations, which offer limited spatial and temporal resolution and do not fully capture shelf-to-slope exchanges. Consequently, there is still a lack of direct observational evidence documenting the transport of dense shelf waters and suspended particulate matter (SPM) from the shelf to the canyon under mild winter conditions, as well as how these events compare to the full spectrum of cascading events observed in the Cap de Creus Canyon. To address this gap, the

present study documents and characterizes a MDSWC event in the Cap de Creus during the mild winter of 2021–2022. We combine hydrographic and velocity measurements collected within the canyon and on the adjacent shelf to investigate the shelf-to-canyon transports, along with reanalysis data to determine the temporal extent of this event and place it in the broader context of cascading events observed in the Cap de Creus Canyon over the past 26 years. By focusing on a mild winter scenario, we aim to provide insights into MDSWC events and discuss the implications for WIW formation and deep-sea ecosystems.

2 Study area

2.1 General setting

The GoL is a micro-tidal river-dominated continental margin that extends from the Cap Croisette Peninsula, in the northern part of the gulf, to the Cap de Creus Peninsula at its southwestern limit (Fig. 1a). It is characterized by a wide continental shelf (up to 70 km) and it is incised by a dense network of submarine canyons (Lastras et al., 2007).

The GoL is impacted by strong continental winds from the north and northwest (Mistral and Tramontane, respectively),

which favor dense water formation and cascading events in winter (Durrieu de Madron et al., 2013) and coastal upwellings in summer (Odic et al., 2022). Humid easterly and southeasterly winds, which blow less frequently, occur primarily from autumn to spring, and can produce large swells and high waves over the continental shelf (Ferré et al., 2008; Leredde et al., 2007; Petrenko et al., 2008; Guizien, 2009). They do not produce a densification of surface waters but they lead to an intense cyclonic circulation on the GoL's shelf and to a strong export of shelf waters at the southwestern exit of the GoL (Ulses et al., 2008a; Mikolajczak et al., 2020).

The ocean circulation of the GoL is also influenced by the freshwater inputs from the Rhône River, one of the largest Mediterranean Rivers, and a series of smaller rivers with typical flash-flooding regimes (Ludwig et al., 2009). The Rhône River supplies an annual river discharge of $1700 \,\mathrm{m}^3 \,\mathrm{s}^{-1}$ and an average of 8.4 Mt yr¹ of suspended particulate matter (Sadaoui et al., 2016; Poulier et al., 2019). The smaller rivers (from south to north the Tech, Têt, Agly, Aude, Orb, Hérault, Lez, and Vidourle) account for slightly 5% of the total inputs of particulate matter ($\sim 0.5 \, \mathrm{Mt \, yr^{-1}}$) to the GoL (Serrat et al., 2001; Bourrin and Durrieu de Madron, 2006). Most of the sediment delivered by these rivers is temporarily stored near their mouths in deltas and prodeltas (Drexler and Nittrouer, 2008), and afterwards it is remobilized and redistributed along the margin by storms and wind-driven alongshelf currents (Estournel et al., 2023). These coastal currents carry particulate material from the shelf towards the southwestern end of the GoL, where the continental shelf rapidly narrows and the Cap de Creus Peninsula constraints the circulation, intensifying the water flow and increasing the particle concentration (Durrieu de Madron et al., 1990; Canals et al., 2006).

The Cap de Creus Canyon represents the limit between the GoL and the Catalan margin (Fig. 1b). The canyon head is located only 4 km from the coast and incises the shelf edge at 110–130 m depth (Lastras et al., 2007). Due to its proximity to the coast and the preferential direction of coastal currents, this canyon has been identified as the main pathway for the transfer of water and sediments from the shelf to the slope and deep margin (Canals et al., 2006; Palanques et al., 2006, 2012).

2.2 Hydrography

The surface layers over the GoL shelf stratify between late spring and autumn (Millot, 1990). In winter, surface cooling and wind-driven mixing weaken the stratification, which lead to a vertically homogeneous water column over the continental shelf (Durrieu de Madron and Panouse, 1996). Offshore, the GoL is characterized by several water masses. The Atlantic Water (AW) fills the upper 250 m and flows into the Mediterranean Sea through the Strait of Gibraltar. During its transit to the GoL, its hydrographic properties undergo chemical and physical modifications, becom-

ing the "old" Atlantic Water (oAW) with T > 13 °C and S = 38.0-38.2 (Millot, 1999). Below, the Eastern Intermediate Water (EIW) occupies the water column between 250 and 850 m depth. It is formed during winter in the Levantine Basin, in the Eastern Mediterranean Sea, by intermediate convection (Font, 1987; Millot, 1999; Taillandier et al., 2022; Schroeder et al., 2024). The Western Mediterranean Deep Water (WMDW) occupies the deepest bathymetric levels and is formed in winter at interannual scales in the GoL by open-ocean deep convection. It typically shows $T \sim 13$ °C and S = 38.43-38.47 (Marshall and Schott, 1999; Somot et al., 2016). During winter, northerly and north-westerly winds cause the formation of dense shelf waters (DSW) over the GoL's shelf (T < 13 °C and S < 38.4) (Houpert et al., 2016; Testor et al., 2018). During mild winters, these dense waters do not gain enough density ($\sigma < 29.1 \,\mathrm{kg}\,\mathrm{m}^{-3}$) to sink into the deep basin, and contribute to the Western Intermediate Water (WIW) $(T = 12.6-13.0 \,^{\circ}\text{C})$ and S = 38.1-38.3body found at upper slope depths (~380-400 m) (Dufau-Julliand et al., 2004; Durrieu de Madron et al., 2005; Juza et al., 2013). The formation of WIW is an important process in the Mediterranean Thermohaline Circulation (MTHC), as it contributes to the ventilation of intermediate layers and plays a role in preconditioning the region for deeper convection events (Juza et al., 2019). During extreme winters, the potential density of DSW exceeds that of the EIW $(\sigma = 29.05 - 29.10 \,\mathrm{kg} \,\mathrm{m}^{-3})$ and even surpasses the density of the WMDW ($\sigma = 29.10-29.16 \text{ kg m}^{-3}$), enabling DSWC to reach the deep basin around 2000-2500 m depth. This process contributes to the ventilation of the deep waters and to the final characteristics of the WMDW (Durrieu de Madron, 2013; Palanques and Puig, 2018).

3 Materials and methods

3.1 Field data

3.1.1 Hydrographic transects and current vertical profiles

During the FARDWO-CCC1 Cruise, onboard the R/V *García del Cid*, two hydrographic transects were conducted on 5–6 March 2022, across the Cap de Creus Canyon, with stations spaced every 1.5 km. The T1 transect covered the upper section of the canyon, while the T2 transect covered the mid-canyon section (Fig. 1b). The hydrographic data were collected using a SeaBird 9 CTD probe coupled with a SeaPoint Fluorometer and Turbidity Sensor (700 nm), an SBE43 dissolved oxygen sensor, and a WetLabs C-Star Transmissometer (650 nm). These sensors were mounted on a rosette system with twelve 12 L Niskin bottles, which collected water samples from various depths. The CTD-Rosette system was hauled through the water column, allowing the comparison of sensor outputs in productive surface waters with high

fluorescence, in clear mid-waters, and in intermediate and bottom nepheloid layers loaded with fine suspended particles. The hydrographic profiles obtained from the CTD stations were interpolated onto a regular grid using the isopycnic gridding method integrated in the Data-Interpolating Variational Analysis (DIVA) gridding software from Ocean Data View (ODV) (v.5.7.2) (Schlitzer, 2023). This method is an advance gridding procedure that aligns property contours along lines of constant potential density (isopycnals) rather than constant depth, which improves the representation of water mass structures and reduces artificial smoothing across density gradients (Schlitzer, 2023). For the interpolation, scale lengths were set to 200 m horizontally and 1 m vertically, with a quality limit of 3.0 and excluding outliers.

Velocity profiles were simultaneously measured using two Lowered Acoustic Doppler Current Profiler (LADCPs) Teledyne 300 kHz narrowband units mounted on the CTD frame. One unit faced upwards and the other downwards to maximize the total range of velocity observations. Each instrument was configured with 20 bins, each 8 m in length, which allowed for a measurement range of $\sim 160\,\mathrm{m}$ (Thurnherr, 2010). The raw LADCP data were processed using the LDEO Software version IX by applying the least-squared method, using the navigation and the vessel-mounted (VM) ADCP data as constraints (Visbeck, 2002).

3.1.2 Vessel-mounted (VM) ADCP data

The R/V García del Cid was equipped with a vessel-mounted (VM) 75 kHz ADCP (Ocean Surveyor, RD Instruments) that recorded current velocities along the hydrographic sections. The VM-ADCP was configured to record current velocities at 2 min averages, while sampling depths were set to 8-m vertical bins. The VM-ADCP data were processed using the CASCADE V7.2 software (Le Bot et al., 2011). Absolute current velocities resulted from removing the vessel speed, derived from a differential global positioning system. The measurement range of the instrument was from 20 to 720 m depth. Given the micro-tidal regime of the Mediterranean Sea (tidal range $\sim 0.5 \,\mathrm{m}$), tides are considered of very low magnitude in the GoL (Davis and Hayes, 1984; Dipper, 2022). Nevertheless, a barotropic tide correction was applied to the VM-ADCP data using the OTIS-TPX8 Tide model (https://www.tpxo.net/global, last access: 1 October 2023) within the cascade V7.2 software, which provided tide-corrected current velocities. VM-ADCP data were then screened to align with the timeframe of the different hydrographic sections. However, the VM-ADCP's range could not fully cover the water column due to the interaction of secondary acoustical lobes with the seabed. To address this limitation, we integrated VM-ADCP data with LADCP measurements recorded at each station. This integration involved aligning time stamps, matching coordinate systems, and merging and interpolating datasets.

Finally, ADCP velocities, decomposed into E–W and N–S components, were rotated 15° counterclockwise to align with the local canyon axis orientation. This rotation provided the across- and along-canyon velocity components for interpretation. For the across-canyon component, eastward velocities have been defined as positive and westward velocities as negative. For the along-canyon component, up-canyon velocities are positive, while down-canyon velocities are negative.

3.1.3 Glider observations

The hydrodynamics of dense shelf waters at the continental shelf adjacent to the Cap de Creus Canyon were monitored by a SeaExplorer underwater glider (ALSEAMAR-ALCEN). The glider carried out one along-shelf (i.e., northsouth) section and navigated 10 km for 25 h, starting on 5 March 2022 (Fig. 1b). It conducted a total of 28 yos (down/up casts). It followed a sawtooth-shaped trajectory through the water column, descending typically to 2 m above the bottom (between 83 and 92 m depth) and ascending to 0-1 m of distance from the surface. The glider was equipped with a pumped SeaBird GPCTD, coupled with a dissolved oxygen sensor (SBE43F), that acquired temperature, conductivity, and pressure data at a sampling rate of 4s. Additionally, the glider had a SeaBird Triplet (WetLabs FLBBCD sensor), which measured proxies of phytoplankton abundance (by measuring the fluorescence of chlorophyll a at 470/695 nm), and total particle concentration (by measuring optical backscattering at 700 nm). Finally, the glider integrated a downward-looking AD2CP (Acoustic Doppler Dual Current Profiler) that measured relative water column velocities and the glider speed. The AD2CP was configured with 15 vertically stacked cells of 2 m resolution, and a sampling frequency of 5 s. Raw velocity measurements were processed using the shear method to derive absolute current velocities (Fischer and Visbeck, 1993; Thurnherr et al., 2015; Homrani et al., 2025). We used bottom tracking and GPS coordinates as constraints to reference each velocity profile. The hydrographic profiles obtained from the glider were similarly interpolated using the isopycnic gridding method as applied to the CTD data (Schlitzer, 2023).

3.2 Ancillary data

3.2.1 Environmental forcings and shelf observational data

Heat flux data were used to evaluate the interaction between the atmosphere and the ocean surface. Data were retrieved from the European Centre for Medium-range Weather Forecast (ECMWF) ERA5 reanalysis by Copernicus Climate Change Service. This global reanalysis product provides hourly estimates of a large number of atmospheric variables since 1940, with a horizontal resolution of 0.25° (Hersbach et al., 2023). For this study, the sea-atmosphere inter-

actions were assessed from 42.6 to 43.4° N and from 3 to 4.5° E, approximately covering the entire GoL's continental shelf, from October 2021 to May 2022.

Significant wave height (H_s) data were retrieved from the Banyuls buoy (06601) located at 42.49° N and 3.17° E (Fig. 1b), through the French CANDHIS database (https: //candhis.cerema.fr, last access: 22 May 2023). These measurements were recorded every 30 min using a directional wave buoy (Datawell DWR MkIII 70). Wind speed and direction data were obtained from the POEM buoy (https://www. seanoe.org/data/00777/88936/, last access: 4 October 2023; Bourrin et al., 2022), which records hourly observations using a surface meteorological sensor and is also equipped with a multiparametric CTD probe measuring near-surface temperature and salinity. In addition, the SOLA station, located in the Bay of Banyuls-sur-Mer (Fig. 1) and managed by the SOMLIT network (https://www.seanoe.org/data/00886/ 99794/, last access: 2 October 2023; Conan et al., 2024) provided weekly near-bottom (~ 27 m) time series of temperature, salinity, and pressure. This data allowed to monitor the presence of dense shelf waters over the continental shelf during the winter of 2021-2022. Raw data were processed to remove gaps and outliers prior to analysis.

Water discharge of rivers opening to the GoL was measured by gauging stations located near rivers mouths and provided by Hydro Portail v3.1.4.3 (https://hydro.eaufrance.fr, last access: 1 October 2023). For this study, we have considered the river discharge from the Rhône River and the total discharge from coastal rivers as the sum of their individual contributions.

3.2.2 Instrumented mooring lines

Current velocity and direction, temperature, and SPM concentration were monitored in two submarine canyons, the Lacaze-Duthiers Canyon (LDC) and the Cap de Creus Canyon (CCC), by means of two instrumented mooring lines (Fig. 1b). The mooring line at Lacaze-Duthiers Canyon, located at about 1000 m depth, has been maintained in the canyon since 1993 as part of the MOOSE program. It is equipped with two current meters (Nortek Aquadopp 2 MHz) with temperature, conductivity, and turbidity sensors, placed at 500 and 1000 m depth (referred to as LDC-500 and LDC-1000, respectively). The sampling interval for the current meters was set to 60 min. The fixed mooring line at the Cap de Creus Canyon has been maintained in the canyon axis by the University of Barcelona since December 2010. This mooring line, referred to as CCC-1000, is equipped with a current meter (Nortek Aquadopp 2 MHz) with temperature, conductivity, and turbidity sensors placed at 18 m above the bottom (mab). The current meter sampling interval was set to 15 min. For this study, the recording period was considered from 1 December 2021 to 1 April 2022, which encompassed the winter of 2021-2022.

3.3 Determination of SPM concentrations from turbidity measurements

To calibrate turbidity measurements obtained in the Cap de Creus Canyon during the FARDWO-CCC1 Cruise, water samples were collected at selected depths with Niskin bottles. For each sample, between 2 and 3 L of water were vacuum filtered into 47 mm 0.4 µm pre-weighted Nucleopore filters. The filters were then rinsed with MiliQ water to remove salt and stored at 4 °C. Then, these filters were dried by desiccation and weighted. The weighing difference of the filters divided by the volume filtered of seawater yielded to the SPM concentration, in $mg L^{-1}$. Finally, the measured SPM concentrations were plotted against in situ turbidity measurements, both from the transmissometer and the optical sensor (Fig. 2a, b). The beam attenuation coefficient (BAC) from the transmissometer showed a stronger correlation with SPM ($R^2 = 0.86$) compared to FTU from the SeaPoint turbidity sensor ($R^2 = 0.81$). Therefore, SPM concentrations were predicted using the equation:

$$SPM = 1.84 \cdot BAC + 0.05(R^2 = 0.85; n = 25)$$
 (1)

Backscatter data (in counts) from a self-contained FLB-BCD optical sensor, identical to the one installed on the Sea-Explorer glider, were also correlated to SPM concentration using a laboratory calibration. Firstly, the optical sensor was submerged into a $10\,L$ plastic tank filled with freshwater. Then, sediment was added while stirring the water to distribute the sediment particles evenly. The amount of sediment was gradually increased until the instrument reached a saturation level of approximately 4000 counts, corresponding to a sediment mass of 447.5 mg. The optical sensor, connected to a computer, displayed and stored the turbidity measurements during the calibration process. Then, water samples were taken at each interval and filtered, obtaining SPM concentration (in mg L^{-1}). Pairs of counts/SPM data points yielded the following regression line (Fig. 2c):

$$SPM = 0.01 \cdot counts(R^2 = 0.97; n = 20)$$
 (2)

Finally, echo intensity (EI) records from the current meters equipped in LDC and CCC lines were also correlated with SPM concentration, using a linear equation relating the logarithm of SPM to EI (Gartner, 2004). Unlike optical devices, acoustic sensors measure relative particle concentrations based on changes on the backscattered acoustic signal (Fugate and Friedrichs, 2002). Acoustic backscatter, expressed in counts, is proportional to the decibel sound pressure level (Lohrmann, 2001), and depends on the particle size and on the operating frequency of the acoustic sensor (Wilson and Hay, 2015). The equation derived from the regression between backscatter data and direct sampling concentration in the GoL was (Fig. 2d):

$$10 \cdot \log(\text{SPM}) = 0.405 \cdot \text{EI} - 22.46 (R^2 = 0.94; n = 66)$$
 (3)

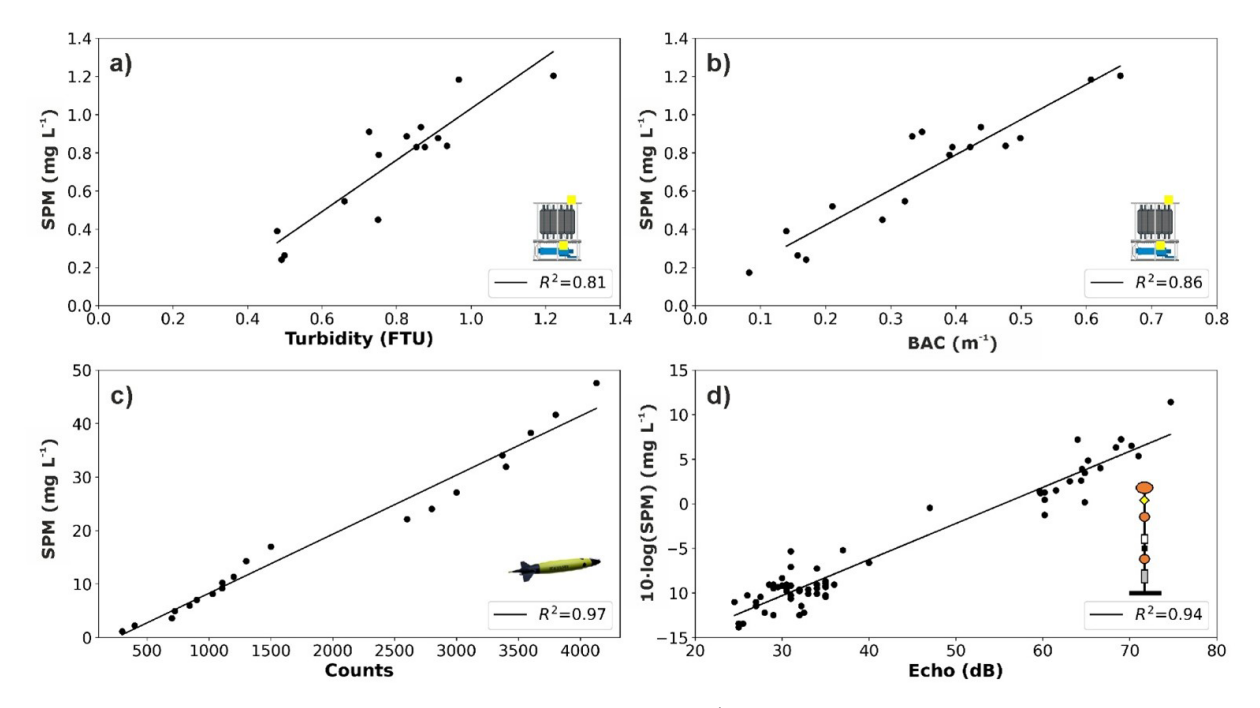


Figure 2. Relationship between the weighed SPM mass concentration (mg L^{-1}) and: (a) turbidity records (FTU) from the SeaPoint sensor and (b) BAC (m⁻¹) from the WetLabs transmissometer attached to the CTD-rosette system; (c) optical backscatter sensor data (counts) from the WetLabs FLBBCD sensor mounted on the SeaExplorer glider; (d) echo intensity (dB) retrieved from the current meters installed in LDC and CCC instrumented moorings. For each relationship, the regression coefficient (R^2) is given.

3.4 Estimation of dense water and SPM transports from observations

The total transports of dense shelf water and associated SPM were estimated using hydrographic and current measurements collected during the FARDWO-CCC1 cruise and the glider survey conducted in early March 2022 in the Cap de Creus Canyon and its adjacent shelf, respectively.

First, to isolate dense shelf waters, we selected water masses with a potential temperature below 12.9 °C and potential density below 29.1 kg m^{-3} . At the canyon, these properties already corresponded to the signature of the Western Intermediate Water (WIW). Then, dense water transports (expressed in Sv = 1×10^6 m³ s⁻¹) were calculated by integrating the zonal component of current speed (which aligns with the down-canyon direction) over the depths occupied by dense shelf waters. For the T1 and T2 transects, current speed was measured using the LADCP attached to the CTDrosette system, and transport was calculated in vertical cells of 8 m (the LADCP bin size) and then integrated over the whole transect. For the glider section over the continental shelf, dense water transport was computed using the same approach, although current velocity data were obtained from the glider-mounted AD2CP.

After estimating dense water transport, we computed the associated SPM transport (in metric tons) by multiplying the calculated water transport by the SPM concentration within the dense water layer. SPM concentrations were derived from

the SeaPoint sensor integrated into the CTD probe for the canyon transects, and from the WetLabs FLBBCD sensor onboard the glider for the shelf section. Finally, all SPM profiles were resampled to match the vertical resolution of current velocity measurements prior to integration.

3.5 Reanalysis data

To complement the observational dataset, we used the Mediterranean Sea Physics Reanalysis (hereafter MedSea) from the Copernicus Marine Service to evaluate the spatiotemporal evolution of hydrographic properties and transport patterns of dense shelf waters in the Cap de Creus Canyon. This reanalysis product has a horizontal resolution of $1/24^{\circ}$ ($\sim 4-5$ km) and provides daily estimates of ocean variables, including temperature, salinity, and currents at multiple depths (Escudier et al., 2020, 2021).

First, we used the MedSea data to assess the temporal evolution of hydrographic conditions during winter 2021–2022. Daily time series of temperature and salinity were extracted from two grid points at key locations along the pathway of dense shelf waters: one located at the shelf break (RA-SB: 42.48° N and 3.29° E, depth = 250 m), and another within the Cap de Creus Canyon (RA-C: 42.34° N and 3.37° E, depth = 350 m) (Fig. 1b).

Then, we calculated the transport of dense shelf waters through the canyon using MedSea data by applying the same approach as for the observational dataset. First, we identified dense shelf waters using the same hydrographic thresholds $(T < 12.9 \,^{\circ}\text{C} \text{ and } \sigma < 29.1 \,\text{kg m}^{-3})$. Then, we estimated the dense water transport (in Sv) by integrating the zonal velocity component (aligned with the downcanyon direction) across two virtual transects close to the T1 and T2 sections sampled during the FARDWO-CCC1 cruise (Fig. 1b). This analysis was performed for the winter of 2021–2022 to capture the temporal variability of the transport, and allowed us to extend the analysis beyond the limited period covered by the field data. Finally, to determine the temporal context and interannual variability of dense shelf water transport, we analyzed a 26-year (1997–2022) time series of MedSea reanalysis data across a central transect in the Cap de Creus Canyon (see location in Fig. 1). Dense shelf waters were identified by temperature < 12.9 °C and zonal velocity > 0.1 m s⁻¹ (down-canyon velocities). We distinguished IDSWC events by a density threshold $> 29.1 \,\mathrm{kg}\,\mathrm{m}^{-3}$, whereas MDSWC events were characterized by densities below this threshold. This long-term analysis allowed us to place the 2021–2022 MDSWC event in the context of other cascading episodes previously reported in the Gulf of Lion and to evaluate its relative intensity.

4 Results

4.1 Meteorological and oceanographic conditions during winter 2021–2022

The meteorological, oceanographic, and hydrological conditions during winter 2021–2022 are summarized in Fig. 3. In order to understand the thermohaline characteristics observed in the Cap de Creus Canyon during the FARDWO-CCC1 cruise in a broader temporal and spatial context, nearbottom temperature, salinity, and potential density at the shelf, shelf break, and canyon for the entire winter of 2021–2022 are also shown in Fig. 3.

The time series of net heat fluxes over the GoL's shelf showed negative values from October 2021 to early April 2022, indicating a heat loss from the ocean to the atmosphere (Fig. 3a). The strongest net heat losses during that winter occurred between November 2021 and late February 2022, reaching values of about $-400 \,\mathrm{W}\,\mathrm{m}^{-2}$ (Fig. 3a). As usual in the study area during winter, the most frequent and generally strongest winds were northern and northwesterly winds (Tramontane and Mistral), alternated with shorter periods of easterly and southeasterly winds (Fig. 3b). The duration of northerly and northwesterly winds varied throughout the season, from short bursts of 1-3 d in October and December to longer periods of 5–7 d in November and February (Fig. 3b), with occasional peaks exceeding 25 m s⁻¹ associated with the strongest heat losses (Fig. 3b, c). A period of sustained northerly winds during February, with wind speeds up to 20 m s⁻¹, preceded and continued through the FARDWO-CCC1 cruise (1–7 March) (Fig. 3b, c). During this period, significant wave height (H_s) ranged between 0.5 and 2.0 m, with no major marine storms recorded before or during the cruise (Fig. 3c). In parallel, the Rhône River discharge displayed average values of about $1850\,\mathrm{m}^3\,\mathrm{s}^{-1}$ (Fig. 3d; Pont et al., 2002; Provansal et al., 2014), while coastal river discharges remained relatively low throughout the entire winter, typically below $200\,\mathrm{m}^3\,\mathrm{s}^{-1}$ (Fig. 3d; Pont et al., 2002; Bourrin and Durrieu de Madron, 2006). This period of strong heat losses, combined with persistent northerly and northwesterly winds, represent the typical winter conditions that favor the formation of dense shelf waters in the Gulf of Lion (Durrieu de Madron et al., 2005).

After the cruise, a series of sustained eastern winds occurred during March and April 2022 (Fig. 3b). From mid-March onwards, easterly winds were more frequent than at any other time of winter 2021–2022 and were particularly intense on 11–13 March, with speeds of $\sim 19 \,\mathrm{m \, s^{-1}}$ (Fig. 3b). In particular, the eastern storm on 13 March was accompanied with $H_s > 3$ m, which lasted for over 20 h (Fig. 3c). The sustained easterly winds during 11-13 March pulled Mediterranean humid air towards southern France, causing intense rainfall from the Eastern Pyrenees to the Massif Central. In contrast, precipitations in the rest of France, including the watershed of the Rhône River, were weak (https:// www.eaufrance.fr/publications/bsh/2022-04, last access: 25 August 2025). As a consequence, coastal river discharges increased up to 2265 m³ s⁻¹, while the Rhône River discharge was comparatively lower (884 m³ s⁻¹) (Fig. 3d).

The hydrographic conditions during winter 2021–2022 revealed the presence of dense shelf waters at the shelf, shelf break and canyon from late January to early March, prior to the FARDWO-CCC1 cruise (Fig. 3e-g). Near-bottom temperature at the continental shelf, measured by the POEM buoy, decreased gradually from 20 to 13 °C during wintertime (Fig. 3e), while salinity fluctuated between 37.8 to 38.1, occasionally dropping below 37.8 in parallel with temperature decreases (Fig. 3f). At the shelf break (250 m depth) and in the Cap de Creus Canyon (350 m depth), reanalysis data showed generally stable thermohaline properties, with short-lived pulses of colder (12.9 °C) waters from late January to early March (Fig. 3e, f). Potential density at the shelf and shelf break increased during February-March 2022 when it peaked at $\sim 28.9 \,\mathrm{kg} \,\mathrm{m}^{-3}$ (Fig. 3g), while density at the canyon remained relatively constant $(28.8-28.95 \text{ kg m}^{-3})$ throughout winter (Fig. 3g).

4.2 Time series at Lacaze-Duthiers and Cap de Creus canyons during winter 2021–2022

Figure 4 shows the time series of temperature, current speed and direction, and SPM concentration recorded at the mooring stations in Lacaze-Duthiers Canyon (at 500 and 1000 m depth) and the Cap de Creus Canyon (at 1000 m depth) during winter 2021–2022. At 500 m depth in Lacaze-Duthiers Canyon (LDC-500), temperature remained relatively constant

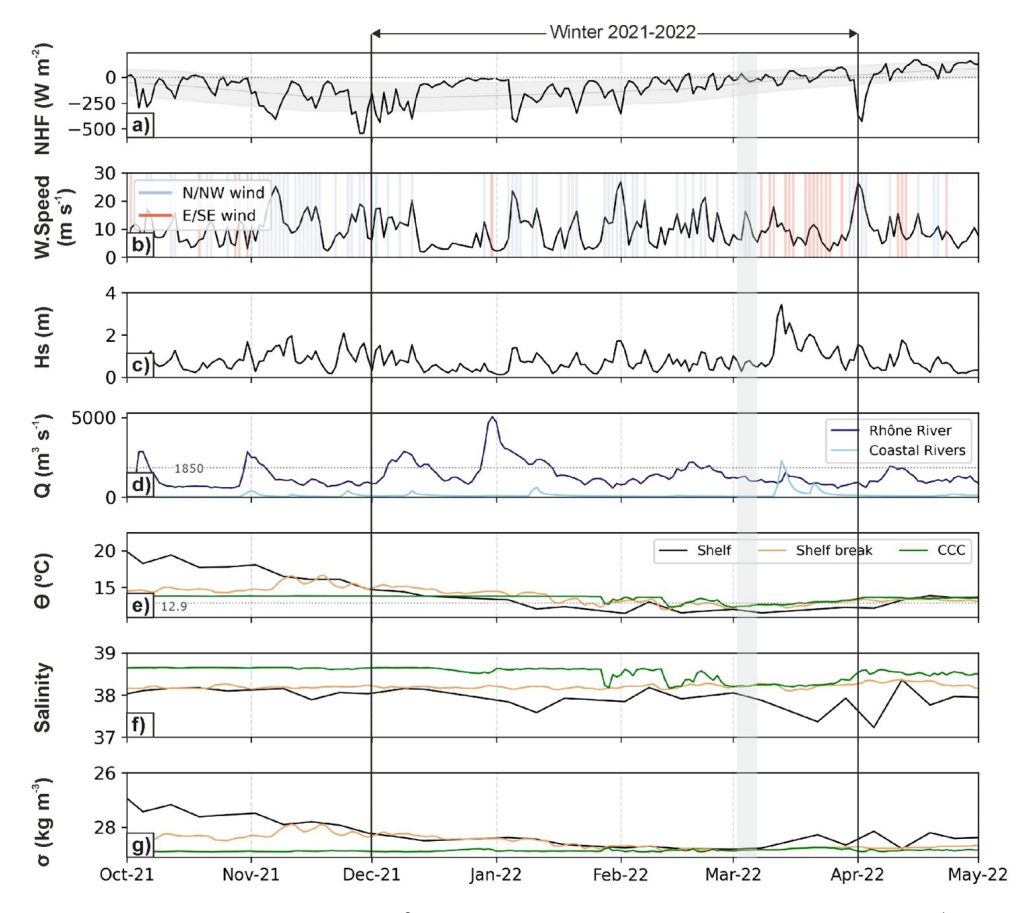


Figure 3. Time series of (a) net heat fluxes (NHF, W m⁻²) averaged over the GoL's shelf; (b) wind speed (m s⁻¹) measured at the POEM buoy. Blue and red shaded bars indicate N/NW and S/SE winds, respectively; (c) significant wave height (H_s , m) measured at the Banyuls buoy; (d) river discharge (Q, m³ s⁻¹) of the Rhône River (dark blue) and coastal river discharges discharging into the GoL (light blue); (e) weekly mean bottom temperature (O, °C), (f) salinity, and (g) potential density (σ , kg m⁻³) calculated from TS data at the continental shelf (black), the shelf break (orange), and the Cap de Creus Canyon (green). Data at the continental shelf were measured at the POEM buoy. Data at the shelf break and within the Cap de Creus Canyon were extracted from two grid points from the MedSea. All data are displayed for the period between October 2021 and May 2022. The grey shaded vertical bar highlights the FARDWO-CCC1 Cruise, which took place on 1–7 March 2022. The studied winter period is also indicated in the figure and corresponds to the time of most negative NHF values, indicating the strongest ocean heat loss to the atmosphere and favorable conditions for DSWC events.

between 13.5 and 14 °C, while at 1000 m in both Lacaze-Duthiers and Cap de Creus canyons, it fluctuated between 13.1 and 13.4 °C (Fig. 4a). Current speeds ranged from 0.01 to 0.1 m s⁻¹ at 500 in Lacaze-Duthiers Canyon and at 1000 m in the Cap de Creus Canyon (Fig. 4b, d), and from 0.1 and $0.2 \,\mathrm{m\,s^{-1}}$ at $1000 \,\mathrm{m}$ in Lacaze-Duthiers Canyon (Fig. 4c). At this depth, current speed increased several times to $0.12\,\mathrm{m\,s^{-1}}$ between January and mid-March 2022, and peaked at 0.2 m s⁻¹ in late March (Fig. 4c). A similar, but less intense peak was observed in the Cap de Creus Canyon at 1000 m during the same period (Fig. 4c), coinciding with small temperature drops (Fig. 4a). Current direction at 500 m in Lacaze-Duthiers Canyon was isotropic (Fig. 4b), while at 1000 m in both Lacaze-Duthiers and Cap de Creus canyons, it became anisotropic and preferentially aligned with the orientation of the respective canyon axes (Fig. 4c, d). SPM concentrations ranged between 0.2 and 0.5 mg L^{-1} at all monitored depths during winter 2021–2022 (Fig. 4e). The highest SPM concentrations were recorded at 1000 m depth in the Cap de Creus Canyon from mid-February to late March 2022, reaching values of $\sim 1 \text{ mg } L^{-1}$ (Fig. 4e). In general, temperature, current speed and direction, and SPM concentrations showed small variability prior to the FARDWO-CCC1 cruise, and the arrival of dense shelf waters was not clearly observed at the monitored depths (Fig. 4).

4.3 Water column properties at the Cap de Creus Canyon and adjacent shelf in March 2022

4.3.1 Hydrographic and biogeochemical properties

The continental shelf adjacent to the Cap de Creus Canyon was monitored on 5 March with a SeaExplorer glider, which

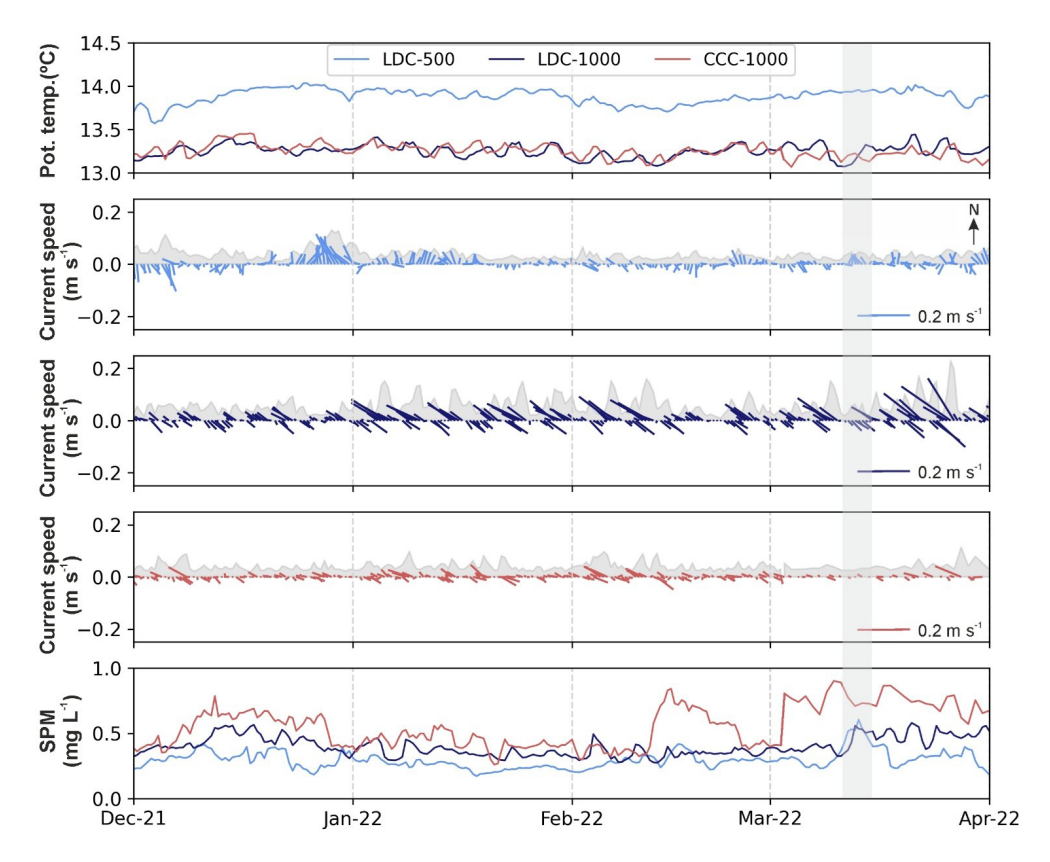


Figure 4. Time series of (a) potential temperature (°C), (b-d) stick plots of currents and current speed as a shaded grey area (m s⁻¹), and (e) suspended particulate matter concentration (SPM, mg L⁻¹) measured at the mooring stations in Lacaze-Duthiers Canyon (LDC-500 in light blue, and LDC-1000 in dark blue) Cap de Creus Canyon (CCC-1000 in red) during winter 2021–2022. In panels (b)–(d), arrows indicate the along-canyon component for each mooring site. The grey shaded vertical bar highlights the FARDWO-CCC1 Cruise, which took place on 1–7 March 2022.

profiled the water column from the surface to 92 m depth. In the northern part of the shelf transect, a water mass characterized by temperatures of 12.9 °C and salinities of 38.2 occupied most of the water column above the $28.95 \,\mathrm{kg}\,\mathrm{m}^{-3}$ isopycnal (Fig. 5a-c). This water mass showed SPM concentrations of 1.5-3.0 mg L⁻¹ and dissolved oxygen values of $\sim 232 \,\mu\text{mol}\,\text{kg}^{-1}$ (Fig. 6a, c). Near the bottom, a cooler, fresher, more turbid, and oxygen-richer water mass was observed in the northern part of the section (Figs. 5ac and 6a-c). This water mass flowed along the shelf below the $28.95 \,\mathrm{kg} \,\mathrm{m}^{-3}$ isopycnal, gradually becoming slightly warmer, saltier, less turbid, and less oxygenated towards the southern shelf (Figs. 5a-c and 6a-c). Fluorescence values also increased southward along the transect (Fig. 6b). Altogether, these hydrographic and biogeochemical properties clearly indicate the presence of dense shelf waters on the continental shelf in the shape of a wedge that thickened towards the Cap de Creus Peninsula (i.e., south) near the bottom (Figs. 5a-c and 6a-c). These conditions represent the oceanographic conditions of the continental shelf shortly before the onset of the FARDWO-CCC1 cruise.

During the FARDWO-CCC1 cruise, two ship-based CTD transects were conducted across the Cap de Creus Canyon. The T1 transect, carried out across the upper canyon, extended from the surface down to 625 m depth. The upper 100 m were characterized by temperatures of 13-13.2 °C, salinities of ~ 38.25 (Fig. 5d, e), dissolved oxygen concentrations of $\sim 200 \,\mu\text{mol kg}^{-1}$, and relatively low SPM concentrations (0.3 mg L^{-1}) (Fig. 6d, f). Beneath this layer, a colder $(12.2-12.7 \,^{\circ}\text{C})$, fresher (S = 38.1-38.2) water mass was observed detaching from the southern flank into the canyon interior at 100-400 m depth (Fig. 5d, f), with densities $\sim 29 \,\mathrm{kg} \,\mathrm{m}^{-3}$, dissolved oxygen values $\sim 200 \,\mathrm{\mu mol} \,\mathrm{kg}^{-1}$), and increased SPM concentrations $(1-1.2 \text{ mg L}^{-1})$ (Fig. 6d– f). Fluorescence values were generally high $(0.5-1.1 \,\mu g \, L^{-1})$ in the upper 400 m of the water column, while they decreased towards the bottom (Fig. 6e). Below, a relatively cooler, saltier, less oxygenated, and slightly denser $(\sim 29.55 \,\mathrm{kg}\,\mathrm{m}^{-3})$ water mass was apparent around 400 m depth (Fig. 5d-f). At depths > 400 m, a much warmer $(T > 13 \,^{\circ}\text{C})$ and saltier $(S \sim 38.4)$ water mass with lower SPM concentrations ($\sim 0.4 \,\mathrm{mg}\,\mathrm{L}^{-1}$) was observed (Figs. 5d– f and 6d–f).

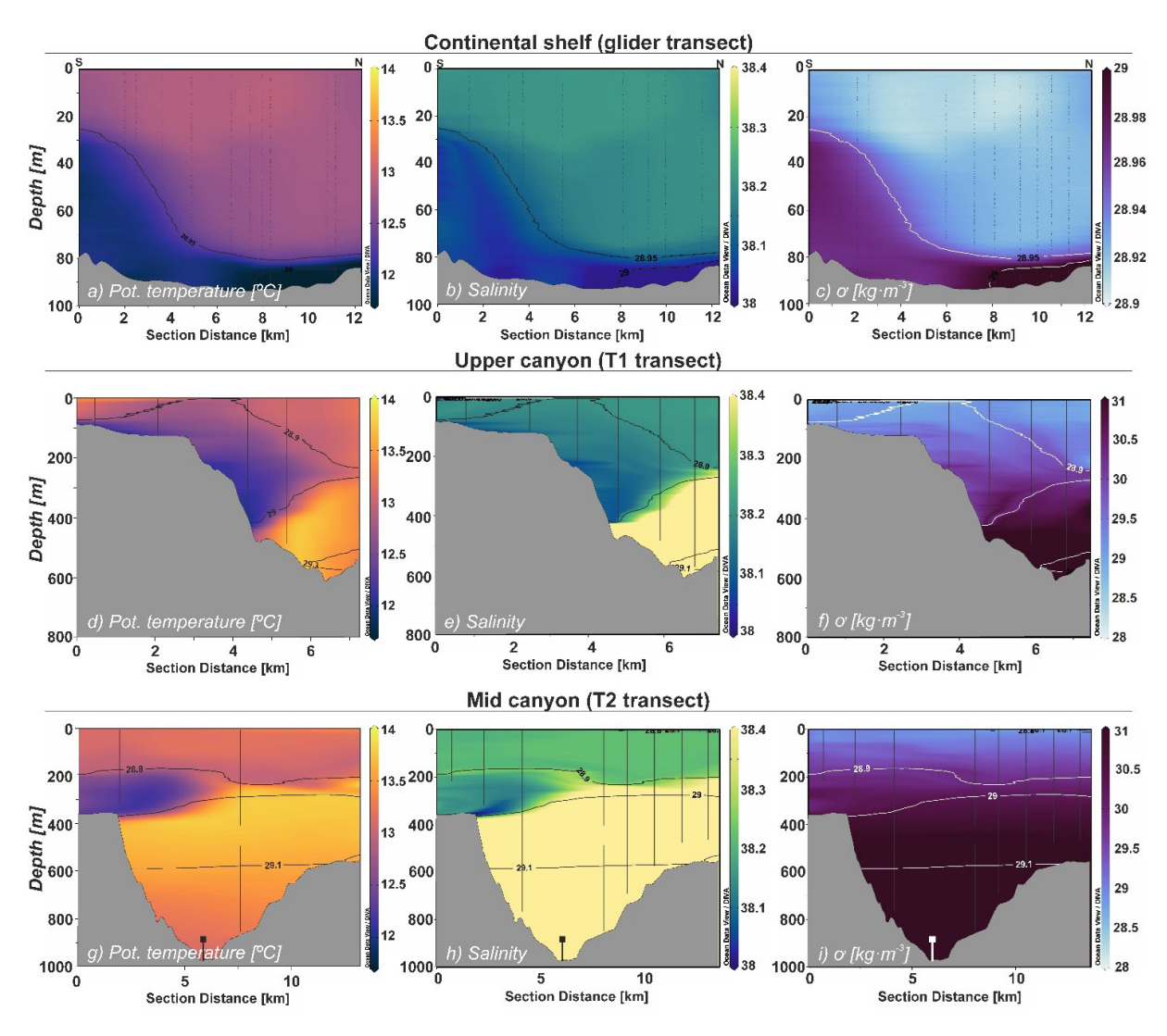


Figure 5. Contour plots of potential temperature (°C), salinity, and potential density $(\sigma, \text{kg m}^{-3})$ at $(\mathbf{a-c})$ the continental shelf (glider transect) and the Cap de Creus Canyon during $(\mathbf{d-f})$ T1 transect and $(\mathbf{g-i})$ T2 transect (FARDWO-CCC1 cruise). Note that for panels (\mathbf{a}) – (\mathbf{c}) , the section distance goes from south to north, whereas for panels (\mathbf{d}) – (\mathbf{i}) , the section distance represents a southwest-northeast direction. Note the change in the density scale in panel (\mathbf{c}) . Figure produced with Ocean Data View $(\mathbf{v}, 5.7.2)$ (Schlitzer, Reiner, Ocean Data View, odv.awi.de, 2023).

Further downcanyon, the T2 transect crossed the middle section of the canyon, covering the water column down to 850 m depth (Figs. 5g–i and 6g–i). The upper 250 m were remarkably homogeneous, with temperatures of 13.2–13.4 °C, salinities of \sim 38.2, dissolved oxygen values \sim 197 µmol kg $^{-1}$, and low SPM concentrations (0.3 mg L $^{-1}$) (Figs. 5g–i and 6g–i). Below, between 250 and 380 m depth, a much colder (12.2–12.3 °C), fresher (38.1), highly oxygenated (200–203 µmol kg $^{-1}$) and moderately turbid (0.8–1.0 mg L $^{-1}$) water mass was observed detaching from the southern canyon flank (Figs. 5g–i and 6g–i). Its density ranged 28.9–29.0 kg m $^{-3}$ (Fig. 5j), and fluorescence values throughout this layer ranged from 0.18 to 0.60 µg L $^{-1}$ (Fig. 6h). Finally, from 400 to 850 m depth, the water column

showed a water mass with temperatures \sim 13.1 °C, salinities of 38.4, and relatively lower oxygen concentrations, fluorescence values, and SPM concentration (Fig. 6g–i).

4.3.2 Currents

At the continental shelf, current velocity measurements indicated a fairly homogeneous current field (Figs. 7a-c). Cross-shelf currents exhibited low velocities ($< 0.1\,\mathrm{m\,s^{-1}}$), predominantly eastward (Fig. 7a), while along-shelf currents were slightly higher ($0.1\text{-}0.15\,\mathrm{m\,s^{-1}}$) and predominantly southward (Fig. 7b). The spatial distribution of currents averaged within the dense water plume (defined between the 28.9 and 29.1 kg m⁻³ isopycnals) shows that dense shelf wa-

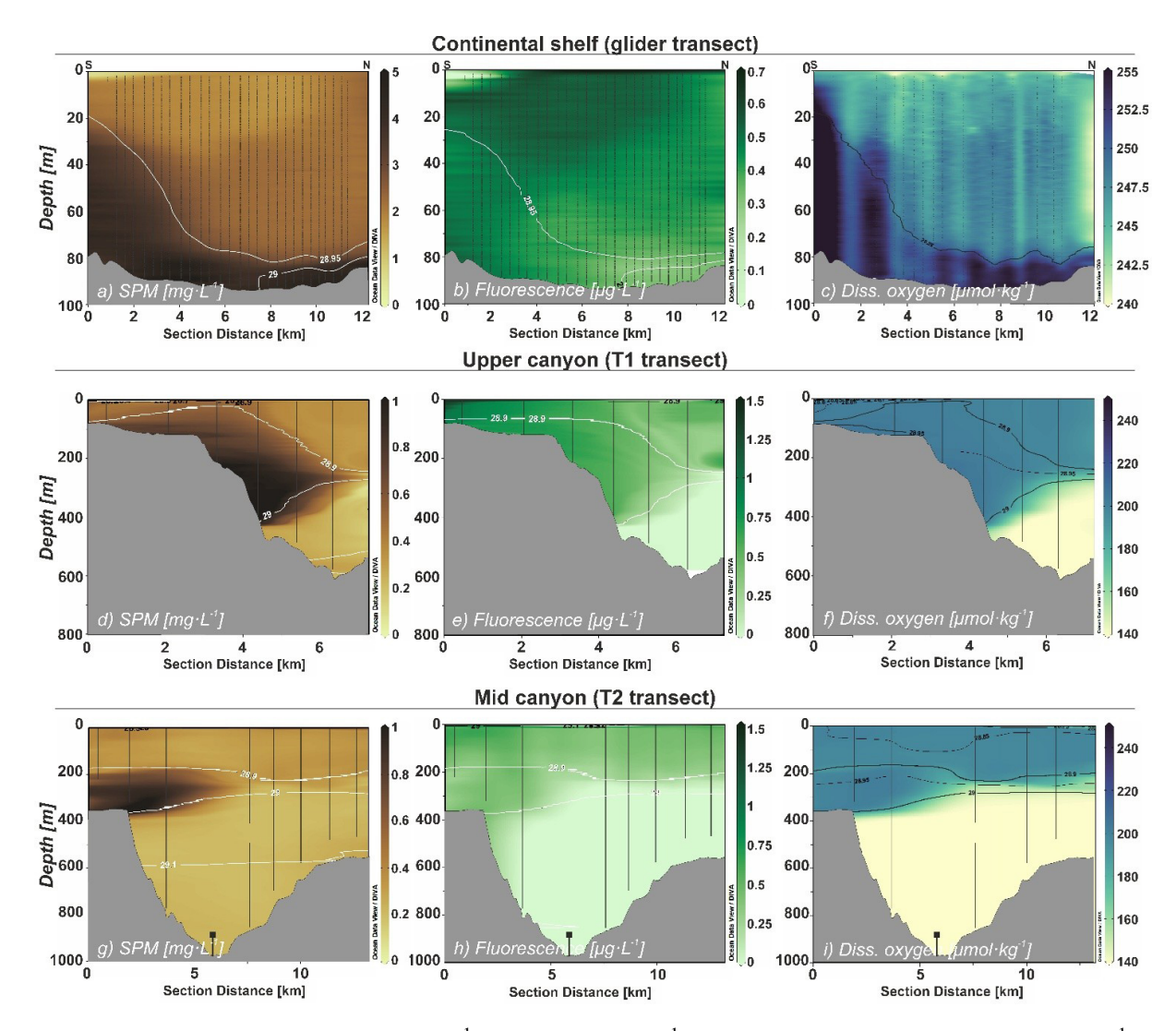


Figure 6. Contour plots of SPM concentration $(mg L^{-1})$, fluorescence $(\mu g L^{-1})$, and dissolved oxygen concentration $(\mu mol kg^{-1})$ at $(\mathbf{a}-\mathbf{c})$ the continental shelf (glider transect) and at the Cap de Creus Canyon during $(\mathbf{d}-\mathbf{f})$ T1 transect and $(\mathbf{g}-\mathbf{i})$ T2 transect (FARDWO-CCC1 cruise). Note that for panels $(\mathbf{a})-(\mathbf{c})$, the section distance goes from south to north, whereas for panels $(\mathbf{d})-(\mathbf{i})$ the section distance represents a southwest-northeast direction. Note the change in the dissolved oxygen scale in panel (\mathbf{c}) . Figure produced with Ocean Data View $(\mathbf{v}. 5.7.2)$ (Schlitzer, Reiner, Ocean Data View, odv.awi.de, 2023).

ters flowed south/south-eastward along the continental shelf adjacent to the Cap de Creus Canyon, with speeds generally around $0.15\,\mathrm{m\,s^{-1}}$ (Fig. 7c). However, in the southern part of the section, currents were stronger, exceeding $0.2\,\mathrm{m\,s^{-1}}$ (Fig. 7c).

In the Cap de Creus Canyon, at the upper section (T1 transect), current velocity measurements revealed the highest speeds from the surface to 400 m depth at the southern canyon flank (Fig. 7d, e). The zonal current velocity (E–W) reached up to $0.3~{\rm m~s^{-1}}$ eastward (Fig. 7d), while the meridional current velocity (N–S) was primarily southward, with velocities between 0.1 and $0.2~{\rm m~s^{-1}}$ (Fig. 7e). These currents appeared relatively confined within the canyon axis, with a pronounced down-canyon component (Fig. 7f). At the

mid-canyon section (T2 transect), the highest current velocities were observed between 200 and 400 m depth (Fig. 7g, h). The zonal current velocities were more pronounced, and reached values of $\sim 0.15~\rm m~s^{-1}$ eastward (Fig. 7g), while the meridional current velocities were slightly smaller, ranging from 0.1 to $0.12~\rm m~s^{-1}$ southward (Fig. 7h). On the southern flank, currents were generally weaker ($\sim 0.1~\rm m~s^{-1}$) and predominantly southward, whereas at the northern canyon flank, these were stronger ($\sim 0.2~\rm m~s^{-1}$) and mainly oriented towards the southeast (Fig. 7i).

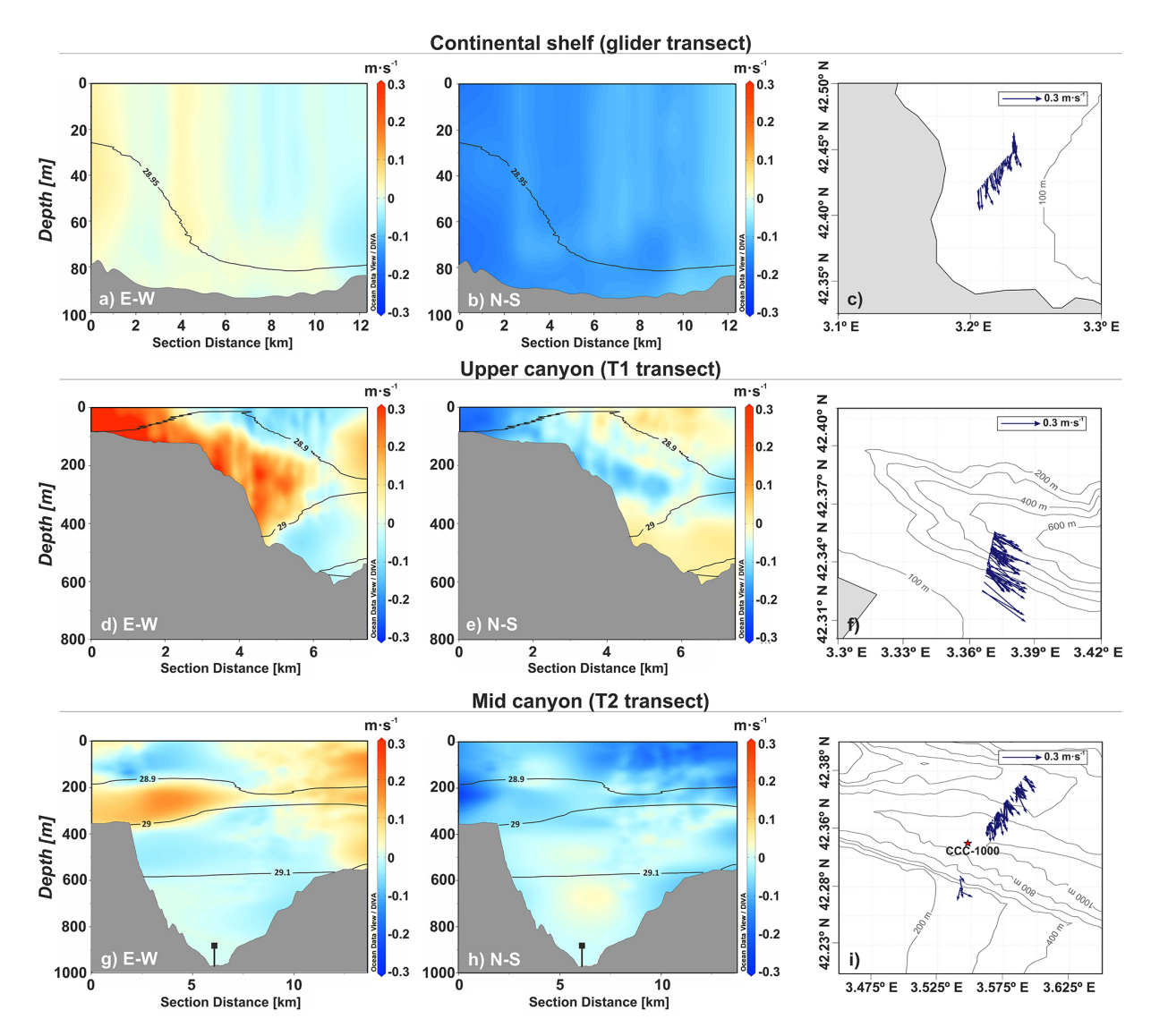


Figure 7. Contour plots of currents measured at (**a**–**b**) the continental shelf (glider transect) and at the Cap de Creus Canyon during (**d**–**e**) T1 transect and (**g**–**h**) T2 transect (FARDWO-CCC1 cruise). Eastward and northward current velocities are positive, while westward and southward current velocities are negative. Panels (**c**), (**f**), and (**i**) display stick plots representing the depth-averaged currents associated with dense waters for the three transects, defined between the 28.9 and 29.05 kg m⁻³ isopycnals. Figure produced with Ocean Data View (v. 5.7.2) (Schlitzer, Reiner, Ocean Data View, odv.awi.de, 2023).

4.4 Duration and magnitude of DSWC during winter 2021–2022

The transports of dense shelf waters and associated SPM in the Cap de Creus Canyon during the observed MDSWC event in March 2022 were 0.7 Sv and 10⁵ t across the continental shelf, 0.3 Sv and 10⁵ t in the upper-canyon, and 0.05 Sv and 10⁴ t in the mid-canyon. Since these observations provided only a snapshot of the event, we used the MedSea reanalysis product to extend our analysis and characterize the temporal evolution and magnitude of cascading events during winter 2021–2022. To do so, we first assessed the reliability of the MedSea by comparing it with our CTD

observations (Fig. A1). In particular, we compared depth-averaged temperatures within the dense water plume (150-400 m depth) at stations where dense waters were detected (Fig. A1), using the root mean square error (RMSE) statistical method. The RMSE were consistently low across all stations (<0.2 °C) (Table A1), indicating a good agreement between both datasets. These results, along with the detailed validation presented in Fos et al. (2025), support the use of the MedSea reanalysis for studying DSWC in this region. In that study, the authors compared the MedSea output with long-term mooring data from the Cap de Creus and Lacaze-Duthiers canyons, and showed that, at 1000 m depth, the

MedSea reproduces 84 % of individual DSWC events within the same week and 56 % on the exact date (Fos et al., 2025).

Based on this validation, we used reanalysis to describe the temporal evolution and magnitude of dense water transports in the Cap de Creus Canyon. Daily MedSea reanalysis indicated that dense water transport was consistently higher in the upper-section than in the mid-canyon throughout winter (Fig. 8a), in agreement with observations. A significant increase in dense water down-canyon transport occurred in late January ($> 0.2 \,\mathrm{Sy}$), coinciding with a drop in temperature $(T < 12.9 \,^{\circ}\text{C})$ and a slight decrease in potential density to 28.85 kg m⁻³ (Fig. 8). Smaller transport (~ 0.12 Sv) was detected in the mid-canyon, but the time series of temperature do not seem to indicate the presence of dense shelf waters in the canyon at that depth (Fig. 9b). Four shallow cascading pulses were further identified in mid- and late February and early March, which had comparable down-canyon transport magnitudes ($\sim 0.2 \, \text{Sv}$) in the upper canyon section (Fig. 8a). The strongest pulse, in mid-March, reached down-canyon transports of ~ 0.4 Sv in the upper canyon and ~ 0.1 Sv in the mid-canyon, accompanied by temperatures around 12 °C and potential densities $\sim 28.9 \,\mathrm{kg} \,\mathrm{m}^{-3}$ (Fig. 8). Occasional upcanyon transports of lower magnitude (~0.1 Sv) were also detected (Fig. 8a), which likely reflect short-term current reversals along the canyon axis (not shown). As March progressed, dense water down-canyon transport gradually decreased, eventually ceasing in early April (Fig. 8a). Accordingly, the cascading season lasted approximately two months (from late January to mid-March), primarily affecting the upper canyon and with weaker influence further downcanyon. After the cascading season, transport shifted predominantly up-canyon (data not shown), reflecting the residual flux along the canyon axis, as previously reported for other canyons of the margin (Martín et al., 2007; Arjona-Camas et al., 2021).

Overall, the total volume of dense shelf waters transported during this period was estimated at $260\,\mathrm{km}^3$ in the upper canyon and $\sim 11\,\mathrm{km}^3$ in the mid-canyon.

5 Discussion

5.1 Forcing conditions during winter 2021–2022

The winter of 2021–2022 was characterized by two distinct periods: an early winter (December–January) with several short northerly and northwesterly windstorms that caused continuous heat losses in the GoL, followed by a late winter (February–March) dominated by eastern storms and lower heat losses (Fig. 3a–c). The mean sea-atmosphere heat loss over the season was $-150\,\mathrm{W}~\mathrm{m}^{-2}$ (Fig. 3a), 25 % lower than typical mild winters in the GoL ($-200\,\mathrm{W}~\mathrm{m}^{-2}$) and half the magnitude of severe winters such as 2004–2005 ($-300\,\mathrm{W}~\mathrm{m}^{-2}$) (Schroeder et al., 2010). From late November to February, several short but intense episodes of heat loss ($\sim 400\,\mathrm{W}~\mathrm{m}^{-2}$) were recorded, peaking in January 2022

(-500 W m⁻²) (Fig. 3a), which likely contributed to significant surface water cooling and buoyancy loss, especially on the inner shelf (Fig. 3e-g). Shelf water temperatures dropped below 12.9 °C in late December/early January and below 12 °C in mid/late February (Fig. 3e), while shelf water densities increased to 28.9–28.95 kg m⁻³, exceeding the prewinter maximum of 27.9 kg m⁻³ (Fig. 9a). These conditions allowed shelf waters formed over the GoL's shelf to spread as a near-bottom layer across the mid and outer shelf and cascade downslope (Figs. 3 and 9b, c). This likely marked the beginning of the MDSWC period, a scenario consistent with previous studies in the GoL (Dufau-Julliand et al., 2004; Durrieu de Madron et al., 2005; Canals et al., 2006; Ulses et al., 2008a).

The cyclonic circulation on the western part of the shelf, driven by the prevailing northerly winds (Ulses et al., 2008a; Bourrin et al., 2008), promoted the transport of these dense shelf waters along the coast (Fig. 9b). The narrowing of the shelf near the Cap de Creus Peninsula further accelerated their overflow into the upper slope, mainly cascading into the westernmost canyons (i.e., Lacaze-Duthiers and Cap de Creus Canyons) (Fig. 9b, c) (Ulses et al., 2008a). According to the MedSea reanalysis, the first cascading pulse in the Cap de Creus Canyon occurred in late January, coinciding with the arrival of cold, dense shelf waters into the upper canyon (Fig. 8). During late winter, especially from late February to late March, four additional cascading pulses occurred in the canyon, the strongest in mid-March (Fig. 8a). This event was strengthened by an eastern storm, which likely enhanced DSWC into the canyon. The role of eastern storms in enhancing DSWC events has been previously documented for the Cap de Creus Canyon in similar studies in the GoL (e.g., Palanques et al., 2008; Ogston et al., 2008; Ribó et al., 2011). Throughout this period, these windstorms were often accompanied with increased freshwater discharge of coastal rivers (Fig. 3d). Such freshwater inputs are commonly observed during mild winters in the region and can locally reduce salinity and density over the shelf (Ulses et al., 2008a; Martín et al., 2013; Mikolajczak et al., 2020), but appeared to have limited impact on shelf water densification during the studied winter (Fig. 3e).

Overall, the mild atmospheric conditions during winter 2021–2022 limited the downslope transport of dense waters into the deeper canyon sections (Fig. 4). As a result, the mild winter of 2021–2022 only generated shallow cascading into the Cap de Creus Canyon (Figs. 5 and 6). The Med-Sea reanalysis further confirmed that dense water transport was consistently higher in the upper canyon than in the mid canyon (Fig. 9a).

5.2 DSWC in the Cap de Creus Canyon in March 2022

During the observational period in early March 2022, one of the shallow cascading pulses previously identified in the MedSea reanalysis (Fig. 8) was directly monitored over the

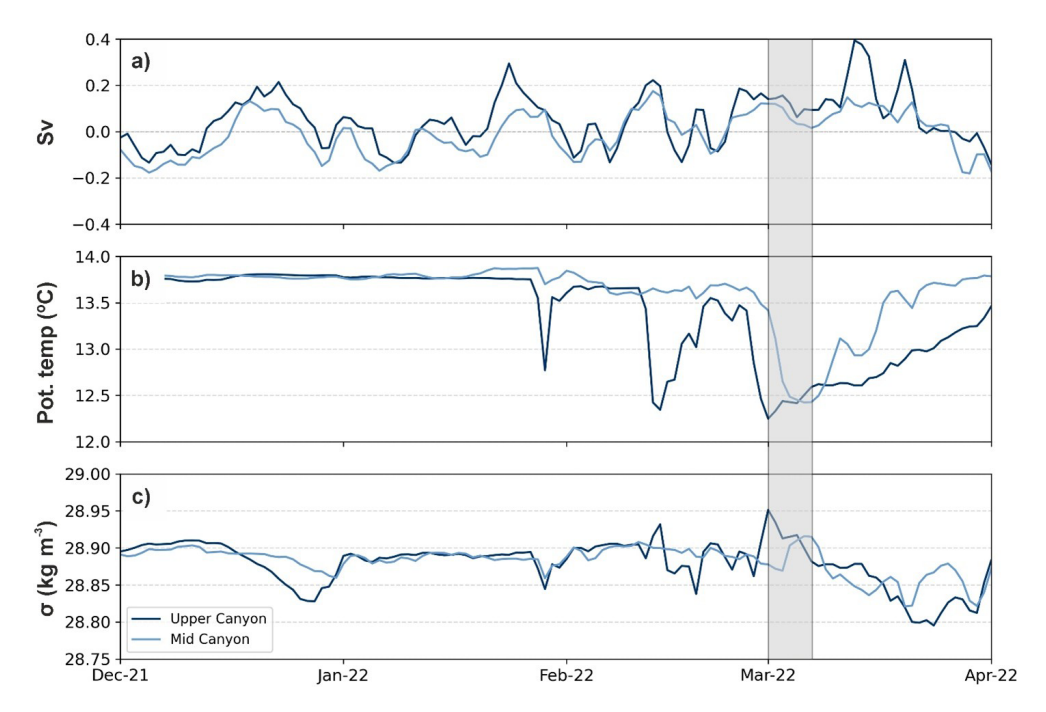


Figure 8. (a) Time series of along-canyon transport (Sv) of dense waters, **(b)** potential temperature (°C), and **(c)** potential density (kg m⁻³) for the upper-canyon transect (dark blue) and the mid-canyon section (light blue), extracted from the Mediterranean Sea Physics Reanalysis product (Escudier et al., 2020, 2021). In panel **(a)**, positive values indicate down-canyon export, while negative values indicate up-canyon export. The grey shaded vertical bar highlights the FARDWO-CCC1 Cruise, which took place on 1–7 March 2022.

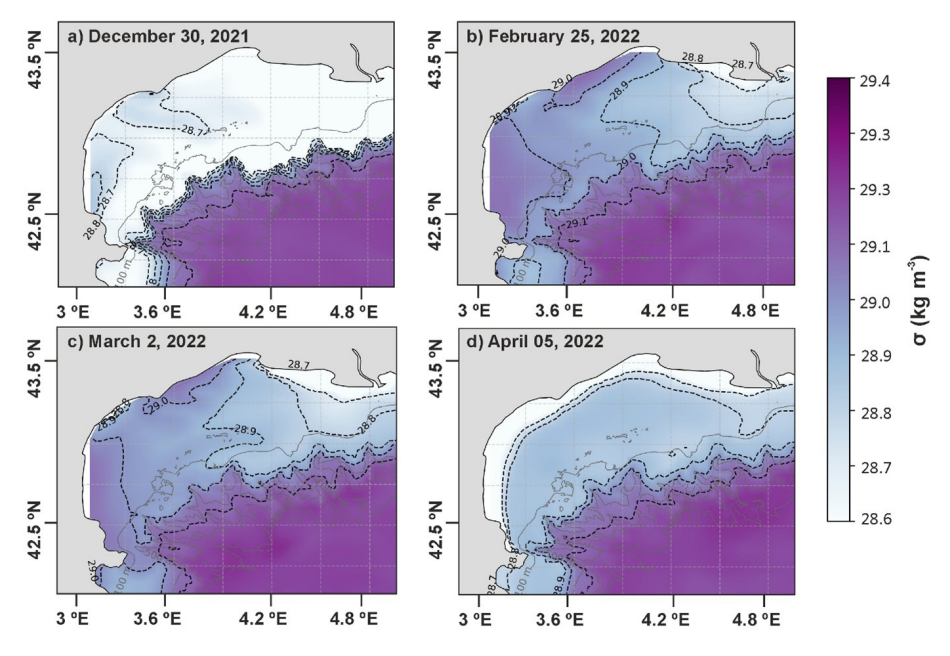


Figure 9. Bathymetric maps of the Gulf of Lion (GoL) showing the potential density anomaly at bottom for four days during the winter of 2021–2022: **(a)** 30 December 2021; **(b)** 25 February 2022; **(c)** 2 March 2022; and **(d)** 5 April 2022. Density contours (black) are displayed every 0.1 kg m⁻³. Data has been obtained from the Mediterranean Sea Physics Reanalysis product (Escudier et al., 2020, 2021).

narrow continental shelf and within the Cap de Creus Canyon (Figs. 5-7). Dense shelf waters were detected over the continental shelf adjacent to the head of the Cap de Creus Canyon (Fig. 5a-c). The steep bathymetry of the inner shelf, combined with the prevailing southwestward currents, facilitated the cascading of dense shelf waters into the canyon head (Dufau-Julliand et al., 2004; Canals et al., 2006; DeGeest et al., 2008). In the upper canyon, dense waters were observed between 100 and 400 m depth (core depth: 380 m), detaching above the EIW ($\sim 400 \,\mathrm{m}$ depth) and contributing to the body of WIW (Figs. 5d-f, 6d-f, and B1). During this cascading event, the dense water plume continued flowing down-canyon to the mid canyon (Fig. 7d-f), where it detached from the southern flank between 250 and 380 m depth and further contributed to the WIW body (Fig. 5g-i). The WIW was likely formed on the outer shelf of the GoL during winter through intense surface cooling and convective mixing of the AW, and then advected southward to the Cap de Creus Canyon by the general circulation (Lapouyade and Durrieu de Madron, 2001; Dufau-Julliand et al., 2004; Juza et al., 2019). Based on the observations during this shallow cascading event, it is plausible that the other events detected in the canyon during this mild winter shared similar characteristics, with dense waters confined to the upper canyon and contributing to the WIW body.

At the mid-canyon, dense waters shifted to a more southward direction compared to the predominantly southeastward direction in the upper canyon (Fig. 7f, i). This flow shift suggests that, as the canyon topography opens, dense waters were no longer constrained by the canyon and veered southward, following the continental slope (Millot, 1990). Previous studies have shown that part of these waters can continue flowing across the Gulf of Roses and reach the neighbouring Palamós and Blanes Canyons (Zúñiga et al., 2009; Ribó et al., 2011). This advection is facilitated by the presence of a shallow NNE-SSW oriented channel that extends from the narrow shelf of the Cap de Creus Canyon to the head of the Palamós Canyon (Durán et al., 2014). During the observed MDSWC event, dense shelf waters and the WIW were likely advected southward through this channel, eventually reaching neighbouring canyons, as documented in previous mild winters (e.g., Arjona-Camas et al., 2021). This southward advection most likely occurred during the other cascading pulses detected in the reanalysis for the studied winter.

In contrast, during extreme winters, dense waters reach potential densities exceeding that of the EIW, generating deep cascading that transports them all the way down canyon (Font et al., 2007; Durrieu de Madron et al., 2013; Palanques and Puig, 2018), rather than following the southward along-slope routes characteristic of MDSWC events.

5.3 Suspended sediment transport during MDSWC events in the Cap de Creus Canyon

During the observational period in early March 2022, MDSWC acted as a pathway to transport SPM and chlorophyll across the continental shelf into the Cap de Creus Canyon (Figs. 5 and 6). Riverine inputs from the Rhône and smaller coastal rivers were low prior to the cruise (Fig. 3d), suggesting that they did not contribute significantly to the increased SPM observed during the event. Conversely, stormwaves and cascading-induced currents were likely the main mechanisms of sediment resuspension and transport. This is consistent with previous findings by Estournel et al. (2023), who documented that, during the mild winter of 2010–2011, storm-induced currents remobilized shelf sediments that subsequently fed the upper section of the Cap de Creus Canyon and along the North Catalan shelf.

Increased SPM and chlorophyll values were mainly observed along the southern canyon flank in both upper and mid canyon, which suggests that dense shelf waters transported phytoplankton cells and contributed additional organic particles to the canyon (Fig. 6d-i). Phytoplankton blooms, which typically peak between December and January, likely provided newly produced biological particles to GoL shelf waters, further enhancing the transport of organic matter into the canyon during this MDSWC event (Fig. B1; Fabres et al., 2008). The preferential accumulation of SPM along the southern canyon flank, contrasting with clear waters on the northern canyon flank, can be explained by the canyon's asymmetric morphology and hydrodynamics. The very narrow adjacent shelf (2.5 km) brings the southern canyon rim close to the coast (Lastras et al., 2007; Durán et al., 2014), where a coastal eddy near the Cap de Creus Peninsula steers dense shelf waters and associated SPM towards the southern flank (Davies et al., 1995; DeGeest et al., 2008). The asymmetric canyon walls reflect this preferential pathway: the northern flank is relatively smooth, with fine-grained silty clays and relatively high accumulation rates (up to $4.1 \,\mathrm{mm}\,\mathrm{yr}^{-1}$), indicative of a depositional area. On the other hand, the southern flank has erosional features, coarser sediments such as gravel, lower accumulation rates $(\sim 0.5 \text{ mm yr}^{-1})$, and oblique furrows interpreted as signatures of DSWC events (Canals et al., 2006: Lastras et al., 2007; DeGeest et al., 2008). Altogether, these morphological and hydrodynamic features likely explain the enhanced SPM concentrations along the southern canyon wall during the observed MDSWC event (Fig. 6d, g).

Although direct observations were limited to the early March event, the other cascading pulses detected in the Med-Sea reanalysis for the same winter probably exhibited similar SPM transport dynamics. During these events, dense shelf waters would have transported SPM along the southern canyon flank to the upper canyon, or exported them southward along the coast. Such behavior resembles transport patterns reported for previous mild winters (Martín et al., 2013;

Estournel et al., 2023). Nevertheless, during the mid-March storm, coastal rivers exhibited a peak in discharge (Fig. 3d), which may have locally enhanced sediment delivery to the canyon, transporting additional SPM during this cascading event.

Overall, it is plausible that the other shallow cascading pulses transported comparable amounts of dense waters and sediments to the canyon, although these estimates remain uncertain due to the lack of direct measurements.

5.4 Interannual variability of dense shelf water transports and future perspectives of DSWC

DSWC in the GoL shows strong interannual variability mainly related to the magnitude and timing of atmospheric forcings (surface heat losses), which ultimately control shelf water densification and, consequently, the magnitude of cascading events, even during mild winters (Herrmann et al., 2008; Mikolajczak et al., 2020). For instance, dense water transports during the mild winters of 2003–2004, 2010– 2011, and 2021–2022 were ~ 75 , ~ 1500 , and $\sim 260 \,\mathrm{km}^3$, respectively, partly reflecting the different net heat losses in those winters $(-125 \,\mathrm{W \, m^{-2}}$ in 2003–2004, $-200 \,\mathrm{W \, m^{-2}}$ in 2010–2011, and $-150 \,\mathrm{W}\,\mathrm{m}^{-2}$ in 2021–2022) (Herrmann et al., 2008; Ulses et al., 2008a; Mikolajczak et al., 2020). During 2003-2004 and 2010-2011, shelf water densities $(\sim 27.78-28.8 \text{ kg m}^{-3})$ were insufficient to generate cascading beyond $\sim 300-350\,\mathrm{m}$ depth and contributed little to the WIW body in the canyon (Ulses et al., 2008a; Martín et al., 2013). In these winters, dense waters did not cascade offshelf, but merely downwelled into the canyon induced by the strong cyclonic circulation during eastern storms and by the subsequent accumulation of seawater along the coast (Martín et al., 2013; Rumín-Caparrós et al., 2013; Mikolajczak et al., 2020). In contrast, in winter 2021–2022, shelf waters reached slightly higher densities ($\sim 28.8-29.1 \,\mathrm{kg}\,\mathrm{m}^{-3}$), cascading further downslope in the upper canyon down to $\sim 400 \, \mathrm{m}$ depth and contributing to the WIW body (Figs. 5 and B1). Nevertheless, downwelling at the canyon head in winter 2010–2011 reached daily magnitudes ($\sim 0.2 \text{ Sy}$ and 10^5 t of SPM; Martín et al., 2013) comparable to the transports during the MDSWC event observed in March 2022. Overall, this illustrates that the intensity and magnitude of DSWC, as well as associated transports, can vary even during mild winters with similar atmospheric characteristics. In comparison, the extreme winter of 2004-2005 was associated with much stronger net heat losses ($\sim -300 \,\mathrm{W \, m^{-2}}$) that led to the formation of very dense shelf waters ($> 29.1 \text{ kg m}^{-3}$) and IDSWC into the deep basin (Canals et al., 2006; Palanques et al., 2006; Ulses et al., 2008a, b; Puig et al., 2013). The total dense water transport during this extreme event was considerably higher than during mild winters, reaching values \sim 1640 km³ (Ulses et al., 2008a). The winters of 2005–2006 and 2011-2012 were also classified as extreme, reflecting similarly strong heat losses and IDSWC events (Palanques et al., 2012; Durrieu de Madron et al., 2013).

Over the past two decades, dense water transport through the Cap de Creus Canyon has shown considerable variability across mild and extreme winters (Fig. 10). According to Mikolajczak et al. (2020), mild winters from the warmest to coldest were 2016–2017, 2010–2011, 2013–2014, and 2015– 2016, with the two warmest years presenting the largest numbers of easterly winds (10-11 d) and, consequently, enhanced dense water transports (Fig. 10). Reanalysis data during winters 2010-2011 and 2016-2017 showed dense waters transports between 0.2–0.4 Sv (Fig. 10). The winter of 2021-2022 experienced 14 d of easterlies, but considering dense water transports, the magnitude of heat losses, and other forcing factors, it would fall between the 2016-2017 and 2010–2011 winters. In contrast, IDSWC events have occurred less frequently, typically every 5-7 years and often in pairs (Fig. 10), and are generally associated with higher dense water transports than MDSWC events, and fewer days of easterlies (~ 1). Extreme winters (from the coldest to the warmest: 2004–2005, 2005–2006, 2011–2012, 2012–2013) (Mikolajczak et al., 2020) showed transports ranging from ~ 0.3 to 0.6 Sv, with the strongest transports occurring in 2004-2005 and 2005-2006 (~ 0.6 Sv), and lower in 2011-2012 ($\sim 0.3 \, \text{Sv}$) and 2012–2013 ($\sim 0.4 \, \text{Sv}$) (Fig. 10). The interannual variability of IDSWC events is likely controlled by intense atmospheric forcing during cold winters, although the precise mechanisms that trigger these events need further analysis (Fos et al., 2025).

However, as shown by the reanalysis time series (Fig. 10) and recent numerical simulations (Mikolajczak et al., 2020), mild and extreme winters can sometimes reach similar magnitudes of dense water transport despite having contrasting atmospheric conditions. For example, during the mild winter of 2010–2011, the total dense water export (1500 km³) was comparable to the extreme winter of 2004–2005 (1640 km³), but the preferential pathways differed. In winter 2010–2011, only 30% of the transport occurred through the canyon, while 70% followed along the coast or remained around the upper canyon. In winter 2004–2005, 69 % of dense shelf water cascaded through the Cap de Creus Canyon down to the deeper parts of the canyon (Ulses et al., 2008a; Mikolajczak et al., 2020). It is very likely that during the winter of 2021–2022, a high proportion of dense waters and associated SPM followed along the coast or southward along the upper slope and canyon. In addition, these findings suggest that during mild winters, MDSWC events may primarily influence coastal ecosystems, whereas during extreme winters, IDSWC may significantly impact deep-benthic ecosystems (Mikolajczak et al., 2020).

Future climate projections indicate an increasing frequency of mild winters in the northwestern Mediterranean (Herrmann et al., 2008; Durrieu de Madron et al., 2023). Under the IPCC-A2 scenario, DSWC could decline by 90 % at the end of the 21st century (Herrmann et al., 2008). This sce-

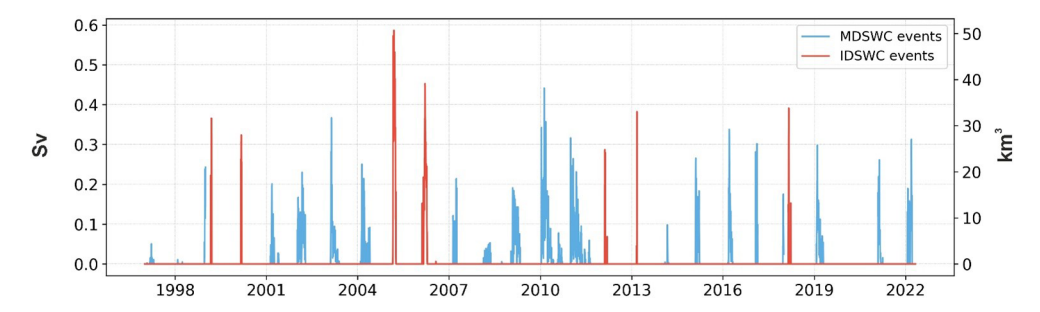


Figure 10. Interannual variability of daily down-canyon transport of dense shelf waters (Sv) from 1997 to 2022, calculated across a central transect in the upper region of the Cap de Creus Canyon (see location in Fig. 1). IDSWC events, defined by densities $> 29.1 \,\mathrm{kg}\,\mathrm{m}^{-3}$, are highlighted in red, whereas mild events, with densities below this threshold, are highlighted in blue. Data have been extracted from the Mediterranean Sea Physics Reanalysis product (Escudier et al., 2020, 2021).

nario would drastically reduce both the intensity and depth penetration of DSWC. Recent studies have already pointed out to a warming and salinification of surface and intermediate waters across the northwestern Mediterranean (Margirier et al., 2020), which would increase the stratification of the water column and hinder deep-ocean convection. Such reduction could strengthen the production of WIW by favouring intermediate-water formation over deep-water ventilation (Parras-Berrocal et al., 2022). Consequently, dense shelf water transport could become more limited to near-coastal areas or upper-canyon regions, altering the regional hydrology and impacting the Mediterranean Thermohaline Circulation (Somot et al., 2006). Ongoing sea warming and increasing stratification are also expected to impact shelf-slope exchanges, reducing IDSWC activity and the associated SPM transports from the GoL to the deep basin (Somot et al., 2006). As a result, the transfer of dense shelf waters and organic matter to the deep sea would be confined to the Catalan shelf or upper Cap de Creus Canyon (Estournel et al., 2023). A decline in the frequency of marine storms could also promote sediment retention in the Rhône River prodelta, reducing the transfer of particulate matter towards the slope and deep basin (Estournel et al., 2023). These changes could significantly modify transport pathways and affect erosion and deposition patterns along the incised submarine canyons of the GoL, and in consequence, have important impacts in deep benthic communities that rely on the arrival of suspended particulate matter. Cold water corals, benthic invertebrates, and commercially important species such as shrimps may be particularly vulnerable, as the limited supply of nutrients and oxygen would hinder their survival (Puig et al., 2001; Pusceddu et al., 2013). In Lacaze-Duthiers Canyon, for instance, Chapron et al. (2020) showed that cold-water coral growth is strongly influenced by the intensity of DSWC events, which modulate their feeding conditions and development. IDSWC events cause high budding rates but low colony linear extension by limiting prey capture rates with high current speeds, whereas MDSWC events cause both high budding rates and linear extension associated with enhanced organic matter supply.

Conversely, the absence of DSWC events can cause high mortality (Chapron et al., 2020). Regardless of the direction of DSWC's effects on deep-sea ecosystems, it has been demonstrated that even a small loss of biodiversity can lead to a major ecosystem collapse (Danovaro et al., 2008), with cascading impacts on ecosystem services such as fisheries (Pörtner and Knust, 2007; Smith et al., 2009).

6 Conclusions

This paper provides a comprehensive observational characterization of a MDSWC event and associated SPM transport in the Cap de Creus Canyon during the mild winter of 2021–2022. We combined glider data, ship-based CTD transects, instrumented mooring lines, and reanalysis data to investigate both the spatial and temporal evolution of shelf-to-canyon transports of dense waters and SPM.

The first part of the winter (December and January) was dominated by several northerly and north-westerly winds that induced sustained heat loss, surface cooling, and densification of surface waters over the GoL, promoting shallow cascading into the Cap de Creus Canyon. Easterly and southeasterly winds dominated the second part of the winter (February and March), and further enhanced shallow cascading into the canyon. In early March 2022, dense shelf waters were observed at the continental shelf during the glider survey. These waters cascaded into the upper canyon down to \sim 400 m depth, where they contributed to the WIW body. Increased SPM concentrations were observed associated with these dense shelf waters, likely indicative of a resuspension process. River discharges were low before and during the cruise and, therefore, they were not the main source of suspended sediments. Instead, storm-waves and cascadinginduced currents likely resuspended and transported SPM through the canyon. We estimated an export of dense water of ~ 0.3 Sv and 10^5 metric tons of sediments in the upper canyon section. Reanalysis data showed that the cascading season in 2021–2022 lasted approximately two months (from late January to mid-March 2022), with several shallow cascading pulses. Peak transport occurred in mid-March associated with an easterly storm that enhanced shallow cascading into the canyon. The total dense water transport over the season was $\sim 260 \, \mathrm{km}^3$. This volume was higher than during the mild winters of 1998-1999 and 2003-2004, but lower than in the mild winter of 2010–2011, highlighting the significant variability of MDSWC even under similar mild atmospheric conditions. Compared with the extreme winter of 2004–2005, the 2021–2022 transport represented roughly half of the total dense water volume transported, further highlighting the variable nature of DSWC in the region. Heat loss seem to be the main factor controlling the density gained by shelf waters during winter, thus the magnitude of the transports. Nevertheless, the exact atmospheric mechanisms driving both MDSWC and IDSWC still deserve further investigation.

Comparison with past events indicates that mild winters can sometimes generate dense water transports comparable in magnitude to those of extreme winters, but the preferential pathways differ. During mild winters, most dense waters flow along the coast or generate shallow cascading to the upper canyon, while in extreme winters, they cascade deep into the canyon and deep basin. It is likely that, during the winter of 2021–2022, a high proportion of dense waters and associated SPM was transported along the coast or generated only shallow cascading into the canyon, resembling previously MDSWC events.

Future research should further investigate the physical dynamics of MDSWC events. More importantly, in the context of climate change, future studies should focus on the evolution and changes on the WIW. These studies would help to understand alterations in the water column properties, stratification and convection processes, and ultimately the impacts on the Mediterranean thermohaline circulation and the functioning of marine ecosystems.

Appendix A: Comparison between in-situ observations and reanalysis data across the Cap de Creus Canyon

Table A1. Comparison of depth-averaged temperatures within the dense water plume derived from observations and reanalysis, with corresponding root mean square errors (RMSE). The location of CTD stations and reanalysis points is shown in Fig. A1.

Stations	Observed temperature (°C)	Reanalysis temperature (°C)	RMSE (°C)
T1-01	12.41	12.42	0.16
T1-02	12.55	12.42	0.17
T1-03	12.34	12.42	0.18
T1-04	12.76	12.46	0.20
T2-01	12.96	12.71	0.15
T2-02	12.68	12.65	0.05
T2-03	12.72	12.65	0.07

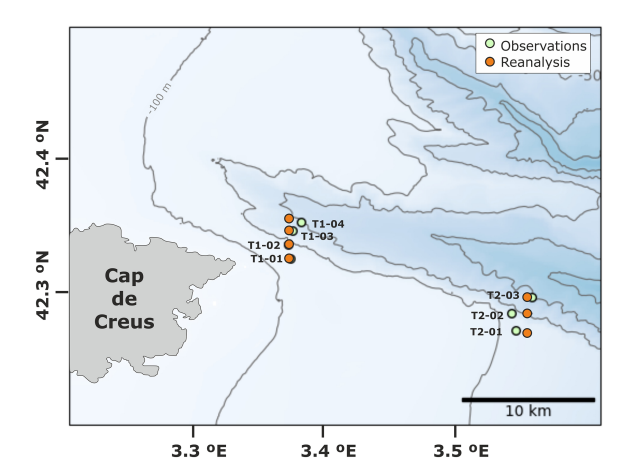


Figure A1. Spatial distribution of CTD stations (green dots) across the Cap de Creus Canyon during the FARDWO-CCC1 cruise where dense shelf waters were observed, and the corresponding MedSea reanalysis grid points (orange dots). Reanalysis data were obtained from the Mediterranean Sea Physics Reanalysis product (Escudier et al., 2020, 2021).

Appendix B: Hydrographic data collected during the FARDWO-CCC1 cruise in the Cap de Creus Canyon and the glider survey on the adjacent continental shelf during March 2022

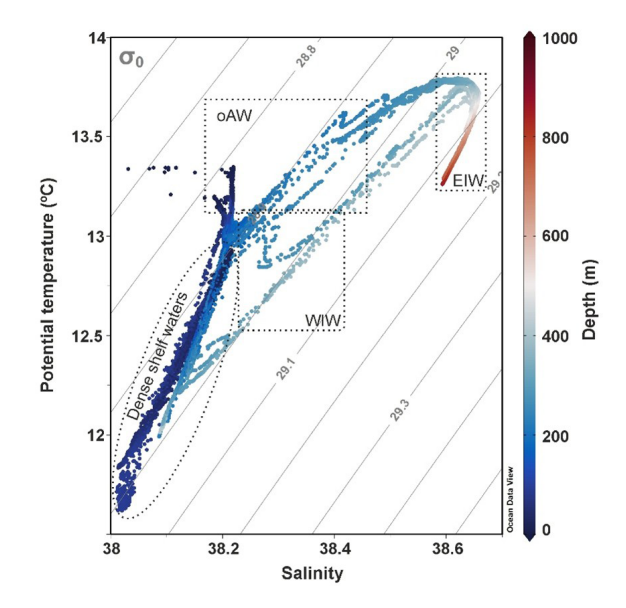


Figure B1. TS diagram from the CTD profiles collected during FARDWO-CCC1 T1 and T2 transects across the Cap de Creus Canyon, as well as those collected during the glider survey at the adjacent shelf (see Fig. 1b for positions). The different water masses that can be identified in the study area are: dense shelf waters, oAW (old Atlantic Water), WIW (Western Intermediate Water), and EIW (Eastern Intermediate Water).

Appendix C: Seasonality of chlorophyll *a* between October 2021 and April 2022 from in situ measurements at the SOLA station

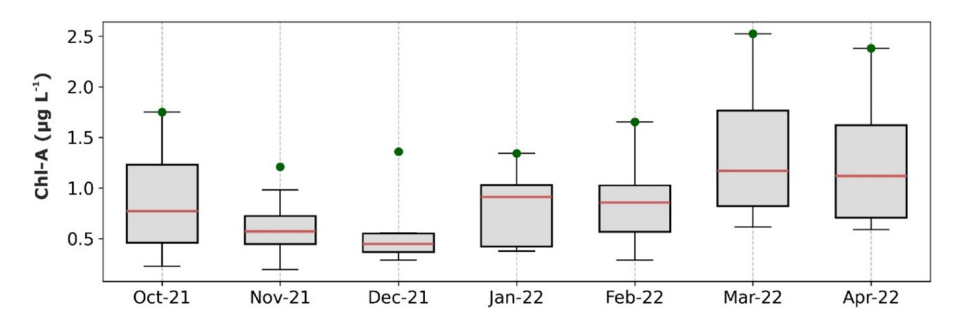


Figure C1. Seasonality of the chlorophyll *a* measured at SOLA station between October 2021 and April 2022. Green dots indicate the monthly maximum values. Data has been retrieved from the SOMLIT-SOLA monitoring site in the Bay of Banyuls-sur-Mer (https://www.seanoe.org/data/00886/99794/, last access: 12 September 2023; Conan et al., 2024).

Data availability. The data that support the findings of this study are publicly available under the following links: SeaExplorer glider from (https://data-selection.odatis-ocean.fr/coriolis/uri/p83112098, last access: 1 April 2023), CCC-1000 moored time series (https://doi.org/10.17882/104746; Sanchez-Vidal et al., 2025a), LDC-500 and LDC-1000 moored time series (https://doi.org/10.17882/45980; Durrieu de Madron et al., 2024). The CTD and the ADCP data collected during the FARDWO-CCC1 Cruise are available at https://doi.org/10.17882/105499 (Sanchez-Vidal et al., 2025b).

Author contributions. AS, DA, XD, and FB defined the research problem, the conce ptualization of the study, and leaded the acquisition of the study data. MA-C carried out the data analysis and produced the figures and first draft of the manuscript. All coauthors discussed the analyses and contributed to the review and writing of the final paper.

Competing interests. The contact author has declared that none of the authors has any competing interests.

Disclaimer. Publisher's note: Copernicus Publications remains neutral with regard to jurisdictional claims made in the text, published maps, institutional affiliations, or any other geographical representation in this paper. While Copernicus Publications makes every effort to include appropriate place names, the final responsibility lies with the authors. Views expressed in the text are those of the authors and do not necessarily reflect the views of the publisher.

Acknowledgements. We are very grateful to the captain, crew, and the scientific team for their dedication and hard work during the FARDWO-CCC1 Cruise at the R/V García del Cid, and to the technicians for their guidance and assistance. We wish to thank the Alseamar Alcen technicians for the glider deployment and piloting, and the data pre-processing. We also want to thank Pascal Conan from OSU-Stamar (Stations Marines UPMC de Banyulssur-Mer) at the Sorbonne Université, as well as acknowledge the MOOSE, the COAST-HF and the SOMLIT programs coordinated by CNRS-INSU and the Research Infrastructure ILICO (CNRS-IFREMER) for providing data from the POEM and SOLA buoys and the Lacaze-Duthiers Canyon's mooring.

Financial support. This work has been supported by the FARDWO project (grant no. PID2020-114322RB-I00) funded by the Ministerio de Ciencia, Innovación y Universidades (grant no. MICI-U/AEI/10.13039/501100011033), the Catalan Government Excellent Research Groups (grant no. 2021 SGR 01195), and the ANR-MELANGE project (grant no. ANR-19-ASMA-0004). MAC was supported by a Margarita Salas postdoctoral grant (2022-2024) from the Ministerio de Universidades of the Spanish Government throughout part of the project. ASV received support from the ICREA program, and HF is supported by the AGAUR FI-SDUR fellowship (grant no. 2023-FISDU-00233) from the Secretaria d'Universitats i Recerca of the Catalan Government.

Review statement. This paper was edited by Ilker Fer and reviewed by Esther Portela Rodriguez and one anonymous referee.

References

- Allen, S. E. and Durrieu de Madron, X.: A review of the role of submarine canyons in deep-ocean exchange with the shelf, Ocean Sci., 5, 607–620, https://doi.org/10.5194/os-5-607-2009, 2009.
- Amblas, D. and Dowdeswell, J. A.: Physiographic influences on dense shelf-water cascading down the Antarctic continental slope, Earth-Sci. Rev., 185, 887–900, https://doi.org/10.1016/j.earscirev.2018.07.014, 2018.
- Arjona-Camas, M., Puig, P., Palanques, A., Durán, R., White, M., Paradis, S., and Emelianov, M.: Natural vs. trawling-induced water turbidity and suspended sediment transport variability within the Palamós Canyon (NW Mediterranean), Mar. Geophys. Res., 42, 38, https://doi.org/10.1007/s11001-021-09457-7, 2021.
- Béthoux, J., Durrieu de Madron, X., Nyffeler, F., and Taiiliez, D.: Deep water in the western Mediterranean: peculiar 1999 and 2000 characteristics, shelf formation hypothesis, variability since 1970 and geochemical interferences, J. Mar. Sys., 33, 117–131, https://doi.org/10.1016/S0924-7963(02)00055-6, 2002.
- Blair, N. E. and Aller, R. C.: The fate of terrestrial organic carbon in the marine environment, Annu. Rev. Mar. Sci., 4, 401–423, https://doi.org/10.1146/annurev-marine-120709-142717, 2012.
- Bourrin, F. and Durrieu de Madron, X.: Contribution to the study of coastal rivers and associated prodeltas to sediment supply in the Gulf of Lions (NW Mediterranean Sea), Life Environ., 56, 307–31, 2006.
- Bourrin, F., Durrieu de Madron, X., Heussner, S., and Estournel, C.: Impact of winter dense water formation on shelf sediment erosion (evidence from the Gulf of Lions, NW Mediterranean), Cont. Shelf Res. 28, 1984–1999, https://doi.org/10.1016/j.csr.2008.06.006, 2008.
- Bourrin, F., Zudaire, L., Vala, T., Vuillemin, R., Conan, P., and Kunesch, S.: POEM Coastal Buoy, SEANOE [data set], https://doi.org/10.17882/88936, 2022.
- Canals, M., Puig, P., Durrieu de Madron, X., Heussner, S., Palanques, A., and Fabres, J.: Flushing submarine canyons, Nature, 444, 354–357, https://doi.org/10.1038/nature05271, 2006.
- Chapron, L., Lebris, N., Durrieu de Madron, X., Peru, E., Galand, P., and Lartaud, F.: Long term monitoring of cold-water coral growth shows response to episodic meteorological events in the NW Mediterranean, Deep Sea Res. I Oceanogr. Pap. 160, 103255, https://doi.org/10.1016/j.dsr.2020.103255, 2020.
- Conan, P., Maria, E., Labatut, P., Zudaire, L., Pujo-Pay, M., Pecqueur, D., Salmeron, C., Crispi, O., Marie, B., and Vuillemin, R.: SOMLIT-SOLA time series (French Research Infrastructure ILICO): long-term core parameter monitoring in the Bay of Banyuls-sur-Mer, SEANOE [data set], https://doi.org/10.17882/99794, 2024.
- Danovaro, R., Gambi, C., Dell'Anno, A., Corinaldesi, C., Fraschetti, S., Vanreusel, A., Vincx, M., and Gooday, A.: Exponential decline of deep-sea ecosystem functioning linked to benthic ecosystem loss, Curr. Biol. 18, 1–18, https://doi.org/10.1016/j.cub.2007.11.056, 2008.
- Davies, P. A., Dakin, J. M., and Falconer, R. A.: Eddy formation behind a coastal headland, J. Coast. Res., 1, 154–167, http://www.jstor.org/stable/4298318 (last access: 25 August 2025), 1995.
- Davis, R. A. and Hayes, M. O.: What is a wave-dominated coast?, Mar. Geol., 60, 313–319, https://doi.org/10.1016/0025-3227(84)90155-5, 1984.

- DeGeest, A. L., Mullenbach, B. L., Puig, P., Nittrouer, C. A., Drexler, T. M., Durrieu de Madron, X., and Orange, D. L.: Sediment accumulation in the western Gulf of Lions, France: the role of Cap de Creus Canyon in linking shelf and slope sediment dispersal systems, Cont. Shelf Res., 28, 2031–2047, https://doi.org/10.1016/j.csr.2008.02.008, 2008.
- Dipper, F.: The seawater environment and ecological adaptations, in: Elements of Marine Ecology, 5th edn., Butterworth-Heinemann, Oxford, UK, 37–151, https://doi.org/10.1016/B978-0-08-102826-1.00002-8, 2022.
- Drexler, T. M. and Nittrouer, C. A.: Stratigraphic signatures due to flood deposition near the Rhône River: Gulf of Lions, northwest Mediterranean Sea, Cont. Shelf Res. 28, 1877–1894, https://doi.org/10.1016/j.csr.2007.11.012, 2008.
- Dufau-Julliand, C., Marsaleix, P., Petrenko, A., and Dekeyser, I.: Three-dimensional modeling of the Gulf of Lion's hydrodynamics (northwest Mediterranean) during January 1999 (MOOGLI3 Experiment) and late winter 1999: Western Mediterranean Intermediate Water's (WIW's) formation and its cascading over the shelf break, J. Geophys. Res. Oceans, 109, https://doi.org/10.1029/2003JC002019, 2004.
- Durán, R., Canals, M., Sanz, J. L., Lastras, G., Amblas, D., and Micallef, A.: Morphology and sediment dynamics of the northern Catalan continental shelf, northwestern Mediterranean Sea, Geomorphology, 204, 1–20, https://doi.org/10.1016/j.geomorph.2012.10.004, 2014.
- Durrieu de Madron, X., Nyffeler, F., and Godet, C. H.: Hydrographic structure and nepheloid spatial distribution in the Gulf of Lions continental margin, Cont. Shelf Res., 10, 915–929, https://doi.org/10.1016/0278-4343(90)90067-V, 1990.
- Durrieu de Madron, X. and Panouse, M.: Transport de matière en suspension sur le plateau continental du Golfe de Lion-Situation estivale et hivernale. Comptes Rendus de l'Académie des Sciences, Série Ila, Paris, 322, 1061–1070, 1996.
- Durrieu de Madron, X., Zervakis, V., Therocharis, A., and Georgopoulos, D.: Comments on "Cascades of dense water around the world ocean", Prog. Oceanogr., 64, 83–90, https://doi.org/10.1016/j.pocean.2004.08.004, 2005.
- Durrieu de Madron, X., Wiberg, P. L., and Puig, P.: Sediment dynamics in the Gulf of Lions: The impact of extreme events, Cont. Shelf Res., 28, 1867–1876, https://doi.org/10.1016/j.csr.2008.08.001, 2008.
- Durrieu de Madron, X., Houpert, L., Puig, P., Sanchez-Vidal, A., Testor, P., Bosse, A., Estournel, C., Somot, S., Bourrin, F., Bouin, M. N., Beauverger, M., Beguery, L., Canals, M., Cassou, C., Coppola, L., Dausse, F., D'Ortenzio, F., Font, J., Heussner, S., Kunesch, S., Lefevre, D., Le Goff, H., Martín, J., Mortier, L., Palanques, A., and Raimbault, P.: Interaction of dense shelf water cascading and open-sea convection in the northwestern Mediterranean during winter 2012, Geophys. Res. Lett. 40, 1379–1385, https://doi.org/10.1002/grl.50331, 2013.
- Durrieu de Madron, X., Aubert, D., Charrière, B., Kunesch, S., Menniti, C., Radakovitch, O., and Sola, J.: Impact of dense water formation on the transfer of particles and trace metals from the coast to the deep in the northwestern Mediterranean, Water, 15, 301, https://doi.org/10.3390/w15020301, 2023.
- Durrieu de Madron, X., Heussner, S., Delsaut, N., Stéphane, K., and Menniti, C.: BILLION observatory data, SEANOE [data set], https://doi.org/10.17882/45980, 2024.

- Escudier, R., Clementi, E., Omar, M., Cipollone, A., Pistoia, J., Aydogdu, A., Drudi, M., Grandi, A., Lyubartsev, V., Lecci, R., Cretí, S., Masina, S., Coppini, G., and Pinardi, N.: Mediterranean Sea Physical Reanalysis (CMEMS MED-Currents) (Version 1), Copernicus Monitoring Environment Marine Service (CMEMS) [data set], https://doi.org./10.25423/CMCC/MEDSEA_MULTIYEAR_PHY_006_004_E3R1, 2020.
- Escudier, R., Clementi, E., Cipollone, A., Pistoia, J., Drudi, M., Grandi, A., Luybartsev, V., Lecci, R., Aydogdu, A., Delrosso, D., Omar, M., Masina, S., Coppini, G., and Pinardi, N.: A high resolution reanalysis for the Mediterranean Sea, Front. Earth Sci., 9, 702285, https://doi.org/10.3389/feart.2021.702285, 2021.
- Estournel, C., Mikolajczak, G., Ulses, C., Bourrin, F., Canals, M., Charmasson, S., Doxaran, D., Duhaut, T., Durrieu de Madron, D., Marsaleix, P., Palanques, A., Puig, P., Radakovitch, O., Sanchez-Vidal, A., and Verney, R.: Sediment dynamics in the Gulf of Lion (NW Mediterranean Sea) during two autumn–winter periods with contrasting meteorological conditions, Prog. Oceanogr., 210, 102942, https://doi.org/10.1016/j.pocean.2022.102942, 2023.
- Fabres, J., Tesi, T., Velez, J., Batista, F., Lee, C., Calafat, A., Heussner, S., Palanques, A., and Miserocchi, S.: Seasonal and event-controlled export of organic matter from the shelf towards the Gulf of Lions continental slope, Cont. Shelf Res., 28, 1971–1983, https://doi.org/10.1016/j.csr.2008.04.010, 2008.
- Ferré, B., Durrieu de Madron, X., Estournel, C., Ulses, C., and Le Corre, G.: Impact of natural (waves and currents) and anthropogenic (trawl) resuspension on the export of particulate matter to the open ocean: application to the Gulf of Lion (NW Mediterranean), Cont. Shelf Res., 28, 2071–2091, https://doi.org/10.1016/j.csr.2008.02.002, 2008.
- Fischer, J. and Visbeck, M.: Deep Velocity Profiling with Self-contained ADCPs, J. Atmos. Ocean. Technol., 10, 764–773, https://doi.org/10.1175/1520-0426(1993)010<0764:DVPWSC>2.0.CO;2, 1993.
- Font, J.: The path of the Levantine intermediate water to the Alboran Sea, Deep Sea Res. I Oceanogr. Res. Pap., 34, 1745–1755, https://doi.org/10.1016/0198-0149(87)90022-7, 1987.
- Font, J., Puig, P., Salat, J., Palanques, A., and Emelianov, M.: Sequence of hydrographic changes in the NW Mediterranean deep water due to the exceptional winter of 2005, Sci. Mar., 71, 339–346, https://doi.org/10.3989/scimar.2007.71n2339, 2007.
- Fos, H., Izquierdo-Peña, J., Amblas, D., Arjona-Camas, M., Romero, L., Estella-Pérez, V., Florindo-Lopez, C., Calafat, A., Cerdà-Domènech, M., Puig, P., Durrieu de Madron, X., and Sanchez-Vidal, A.: Solving dense shelf water cascading with a high-resolution ocean reanalysis, ESS Open Archive, 17 March, https://doi.org/10.22541/essoar.174060515.57729804/v2, 2025.
- Fugate, D. C. and Friedrichs, C. T.: Determining concentration and fall velocity of estuarine particle populations using ADV, OBS and LISST, Cont. Shelf Res., 22,, 1867–1886, https://doi.org/10.1016/S0278-4343(02)00043-2, 2002.
- Gales, J., Rebesco, M., De Santis, L., Bergamasco, A., Colleoni, F., Kim S., Accetella, A., Kovacevic, V., Liu, Y., Olivo, E., Colizza, E., Florindo-Lopez, C., Zgur, F., and McKay, R.: Role of dense shelf water in the development of Antarctic submarine canyon morphology, Geomorphology, 372, 107453, https://doi.org/10.1016/j.geomorph.2020.107453, 2021.

- Gartner, J. W.: Estimating suspended soils concentrations from backscatter intensity measured by acoustic Doppler current profiler in San Francisco Bay, California, Mar. Geol., 211, 169–187, https://doi.org/10.1016/j.margeo.2004.07.001, 2004.
- Guizien, H.: Spatial variability of wave conditions in the Gulf of Lions (NW Mediterranean Sea), Vie et Milieu/Life & Environment, 261–270, https://hal.sorbonne-universite.fr/hal-03253740v1 (last access: 24 November 2025), 2009.
- Herrmann, M., Estournel, C., Déqué, M., Marsaleix, P., Sevault, F., and Somot, S.: Dense water formation in the Gulf of Lions shelf: Impact of atmospheric interannual variability and climate change, Cont. Shelf Res., 28, 2092–2112, https://doi.org/10.1016/j.csr.2008.03.003, 2008.
- Hersbach, H., Bell, B., Berrisford, P., Biavati, G., Horányi, A., Muñoz Sabater, J., Nicolas, J., Peubey, C., Radu, R., Rozum, I., Schepers, D., Simmons, A., Soci, C., Dee, D., and Thépaut, J.-N.: ERA5 hourly data on pressure levels from 1940 to present. Copernicus Climate Change Service (C3S) Climate Data Store (CDS) [data set], https://doi.org/10.24381/cds.bd0915c6, 2023.
- Heussner, S., Durrieu de Madron, X., Calafat, A., Canals, M., Carbonne, J., Desault, N., and Saragoni, G.: Spatial and temporal variability of downward particle fluxes on a continental slope: lessons from an 8-yr experiment in the Gulf of Lions (NW Mediterranean), Mar. Geol., 234, 63–92, https://doi.org/10.1016/j.margeo.2006.09.003, 2006.
- Homrani, S., Pasqueron de Fommervault, O., Gentil, M., Jourdin, F., Durieu de Madron, X., and Bourrin, F.: Tracing suspended sediment fluxes using a glider: observations in a tidal shelf environment, EGUsphere [preprint], https://doi.org/10.5194/egusphere-2024-4072, 2025.
- Houpert, L., Durrieu de Madron, X., Testor, P., Bosse, A., D'Ortenzio, F., Bouin, M. N., Dausse, D., Le Goff, H., Kunesch, S., Labaste, M., Coppola, L., Mortier, L., and Raimbault, P.: Observations of open-ocean deep convection in the northwestern Mediterranean Sea: Seasonal and interannual variability of mixing and deep water masses for the 2007–2013 Period, J. Geophys. Res. Oceans, 121, 8139–8171, https://doi.org/10.1002/2016JC011857, 2016.
- Ivanov, V. V., Shapiro, G. I., Huthnance, J. M., Aleynik, D. L., and Golovin, P. N.: Cascades of dense water around the world, Progr. Oceanogr., 60, 47–98, https://doi.org/10.1016/j.pocean.2003.12.002, 2004.
- Kwon, E., DeVries, T., Galbraith, E. D., Hwang, J., Kim, G., and Timmermann, A.: Stable carbon isotopes suggest large terrestrial carbon inputs to the global ocean, Global Biogeochem. Cycles, 35, e2020GB006684, https://doi.org/10.1029/2020GB006684, 2021.
- Juza, M., Renault, L., Ruiz, S., and Tintoré, J.: Origin and pathways of Winter Intermediate Water in the Northwestern Mediterranean Sea using observations and numerical simulation, J. Geophys. Res., 118, 6621–6633, https://doi.org/10.1002/2013JC009231, 2013.
- Juza, M., Escudier, R., Vargas-Yáñwz, M., Mourre, B., Heslop, E., Allen, J., and Tintoré, J.: Characterization of changes in Western Intermediate Water properties enabled by an innovative geometry-based detection approach, J. Mar. Sys., 191, 1–12, https://doi.org/10.1016/j.jmarsys.2018.11.003, 2019.
- Lastras, G., Canals, M., Urgeles, R., Amblas, D., Ivanov, M., Droz, L., Dennielou, B., Fabrés, J., Schoolmeester,

- T., Akhmetzhanov, A., Orange, D., and García-García, A.: A walk down the Cap de Creus Canyon, Northwestern Mediterranean Sea: Recent processes inferred from morphology and sediment bedforms, Mar. Geol., 246, 176–192, https://doi.org/10.1016/j.margeo.2007.09.002, 2007.
- Lapouyade, A. and Durrieu de Madron, X.: Seasonal variability of the advective transport of particulate and organic carbon in the Gulf of Lion (NW Mediterranean), Oceanol. Acta, 24, 295=-312, https://doi.org/10.1016/S0399-1784(01)01148-3, 2001.
- Le Bot, P., Kermabon, C., Lherminier, P., and Gaillard, F.: CAS-CADE V6.1: Logiciel de validation et de visualisation des mesures ADCP de coque. Rapport technique OPS/LPO 11-01. Ifremer, Centre de Brest, France, https://archimer.ifremer.fr/doc/00342/45285/ (last access: 24 November 2025), 2011.
- Leredde, Y., Denamiel, C., Brambilla, E., Lauer-Leredde, C., Bouchette, F., and Marsaleix, P.: Hydodynamics in the Gulf of Aigues-Mortes, NW Mediterranean Sea: In situ and modelling data, Cont. Shelf Res., 27, 2389–2406, https://doi.org/10.1016/j.csr.2007.06.006, 2007.
- Levin, L. A. and Sibuet, M.: Understanding continental margin biodiversity: a new imperative, Annu. Rev. Mar. Sci., 4, 79–112, https://doi.org/10.1146/annurev-marine-120709-142714, 2012.
- Liu, Z., Zhao, Y., Colin, C., Stattegger, K., Wiesner, M. G., Huh, C. A., Zhang, Y., Li, X., Sompongchaiyakul, P., You, C. F., Huany, C., Liu, J. T., Siringan, F. P., Le, Sathiamurthy, E., Hantoro, W. S., Liu, J., Tuo, S., Zhao, S., Zhou, S., He, Z., Wang, Y., Bunsomboonsakul, S., and Li, Y.: Source-to-sink transport processes of fluvial sediments in the South China Sea, Earth Sci. Rev. 153, 238–273, https://doi.org/10.1016/j.earscirev.2015.08.005, 2016.
- Lohrmann, A.: Monitoring Sediment Concentration with Acoustic Backscattering Instruments, Nortek, https://www.nortekgroup.com/assets/documents/Monitoring-sediment-concentration-with-acoustic-backscattering-instruments.pdf (last access: 1 April 2023), 2001.
- Ludwig, W., Dumont, E., Meybeck, M., and Heussner, S.: River discharges of water and nutrients to the Mediterranean and Black Sea: major drivers for ecosystem changes during past and future decades?, Prog. Oceanogr., 80, 199–217, https://doi.org/10.1016/j.pocean.2009.02.001, 2009.
- Mahjabin, T., Pattiaratchi, C., Hetzel, Y., and Janekovic, I.: Spatial and temporal variability of dense shelf water cascades along the Rottnest continental shelf in southwest Australia, J. Mar. Sci. Eng., 7, 30, https://doi.org/10.3390/jmse7020030, 2019.
- Mahjabin, T., Pattiaratchi, C., and Hetzel, Y.: Occurrence and seasonal variability of Dense Shelf Water Cascades along Australian continental shelves, Sci. Rep., 10, 9732, https://doi.org/10.1038/s41598-020-66711-5, 2020.
- Margirier, F., Testor, P., Heslop, E., Mallil, K., Bosse, A., Houpert, L., Mortier, L., Bouin, M., Coppola, L., D'Ortenzio, F., Durrieu de Madron, X., Mourre, B., Prieur, L., Raimbault, P., and Taillandier, V.: Abrupt warming and salinification of intermediate waters interplays with decline of deep convection in the Northwestern Mediterranean Sea, Sci. Rep., 10, 20923, https://doi.org/10.1038/s41598-020-77859-5, 2020.
- Marshall, J. and Schott, F.: Open-ocean convection: Observations, theory, and models, Rev. Geophys., 37, 1–64, https://doi.org/10.1029/98RG02739, 1999.
- Martín, J., Palanques, A. and Puig, P.: Near-bottom horizontal transfer of particulate matter in the Palamós submarine canyon (NW

- Mediterranean), J. Mar. Res., 65, 193–218, https://elischolar.library.yale.edu/journal_of_marine_research/163 (last access: 24 November 2025), 2007.
- Martín, J., Durrieu de Madron, X., Puig, P., Bourrin, F., Palanques, A., Houpert, L., Higueras, M., Sanchez-Vidal, A., Calafat, A. M., Canals, M., Heussner, S., Delsaut, N., and Sotin, C.: Sediment transport along the Cap de Creus Canyon flank during a mild, wet winter, Biogeosciences, 10, 3221–3239, https://doi.org/10.5194/bg-10-3221-2013, 2013.
- Mikolajczak, G., Estournel, C., Ulses, C., Marsaleix, P., Bourrin, F., Martín, J., Pairaud, I., Puig, P., Leredde, Y., Many, G., Seyfried, L., and Durrieu de Madron, X.: Impact of storms on residence times and export of coastal waters during a mild autumn/winter period in the Gulf of Lion, Cont. Shelf Res., 207, 104192, https://doi.org/10.1016/j.csr.2020.104192, 2020.
- Millot, C.: The Gulf of Lions' hydrodynamics, Cont. Shelf Res., 10, 885–894, https://doi.org/10.1016/0278-4343(90)90065-T, 1990.
- Millot, C.: Circulation in the Western Mediterranean, J. Mar. Syst., 20, 423–442, https://doi.org/10.1016/S0924-7963(98)00078-5, 1999.
- Nittrouer, C. A., Austin, J. A., Field, M. E., Kravitz, J. H., Syvitski, J. P., and Wiberg, P. L.: Continental margin sedimentation: from sediment transport to sequence stratigraphy, John Wiley and Sons, https://doi.org/10.1002/9781444304398, 2009.
- Odic, R., Bensoussan, N., Pinazo, C., Taupier-Letage, I., and Rossi, V.: Sporadic wind-driven upwelling/down-welling and associated cooling/warming along Northwestern Mediterranean coastlines, Cont. Shelf Res., 250, 104843, https://doi.org/10.1016/j.csr.2022.104843, 2022.
- Ogston, A. S., Drexler, T. M., and Puig, P.: Sediment delivery, resuspension, and transport in two contrasting canyon environments in the southwest Gulf of Lions, Cont. Shelf Res., 28, 2000–2016, https://doi.org/10.1016/j.csr.2008.02.012, 2008.
- Palanques, A., Durrieu de Madron, X., Puig, P., Fabrés, J., Guillén, J., Calafat, A., Canals, M., Heussner, S., and Bonnin, J.: Suspended sediment fluxes in the Gulf of Lions submarine canyons. The role of storms and dense water cascading, Mar. Geol., 234, 43–61, https://doi.org/10.1016/j.margeo.2006.09.002, 2006.
- Palanques, A., Guillén, J., Puig, P., and Durrieu de Madron, X.: Storm-driven shelf-to-canyon suspended sediment transport at the southwestern Gulf of Lions, Cont. Shelf Res., 28, 1947–1956, https://doi.org/10.1016/j.csr.2008.03.020, 2008.
- Palanques, A., Puig, P., Durrieu de Madron, X., Sanchez-Vidal, A., Pasqual, C., Martín, J., Calafat, A., Heussner, S., and Canals, M.: Sediment transport to the deep canyons and open-slope of the western Gulf of Lions during the 2006 intense cascading and open-sea convection period, Prog. Oceanogr., 106, 1–15, https://doi.org/10.1016/j.pocean.2012.05.002, 2012.
- Palanques, A. and Puig, P.: Particle fluxes induced by benthic storms during the 2012 dense shelf water cascading and open sea convection period in the northwestern Mediterranean Basin, Mar. Geol., 406, 119–131, https://doi.org/10.1016/j.margeo.2018.09.010, 2018.
- Parras-Berrocal, I. M., Vázquez, R., Cabos, W., Sein, D. V., Álvarez, O., Bruno, M., and Izquierdo, A.: Surface and intermediate water changes triggering the future collapse of deep water formation in the North Western Mediterranean, Geophys. Res. Lett., 49, e2021GL095404, https://doi.org/10.1029/2021GL095404, 2022.

- Pasqual, C., Sanchez-Vidal, A., Zúñiga, D., Calafat, A., Canals, M., Durrieu de Madron, X., Puig, P., Heussner, S., Palanques, A., and Delsaut, N.: Flux and composition of settling particles across the continental margin of the Gulf of Lion: the role of dense shelf water cascading, Biogeosciences, 7, 217–231, https://doi.org/10.5194/bg-7-217-2010, 2010.
- Petrenko, A., Dufau, C., and Estournel, C.: Barotropic eastward currents in the western Gulf of Lion, north-western Mediterranean Sea, during stratified conditions, J. Mar. Syst., 74, 406–428, https://doi.org/10.1016/j.jmarsys.2008.03.004, 2008.
- Pont, D., Simonnet, J. P., and Walter, A. V.: Medium-term changes in suspended sediment delivery to the ocean: consequences of catchment heterogeneity and river management (Rhône River, France), Estuar. Coast. Shelf Sci., 54, 1–18, https://doi.org/10.1006/ecss.2001.0829, 2002.
- Pörtner, H. O. and Knust, R.: Climate change affects marine fishes through oxygen limitation of thermal tolerance, Science, 315, 95–97, https://doi.org/10.1126/science.1135471, 2007.
- Poulier, G., Launay, M., Le Bescond, C., Thollet, F., Coquery, M., and Le Coz, J.: Combining flux monitoring and data reconstruction to establish annual budgets of suspended particulate matter, mercury and PCB in the Rhône River from Lake Geneva to the Mediterranean Sea, Sci. Total Environ., 658, 457–273, https://doi.org/10.1016/j.scitotenv.2018.12.075, 2019.
- Provansal, M., Dufour, S., Sabatier, F., Anthony, E. J., Raccasi, G., and Robresco, S.: The geomorphic evolution and sediment balance of the lower Rhône River (southern France) over the last 130 years: Hydropower dams versus other control factors, Geomorphology, 219, 27–41, https://doi.org/10.1016/j.geomorph.2014.04.033, 2014.
- Puig, P., Durrieu de Madron, X., Salat, J., Schroeder, K., Martín, J., Karageorgis, A. P., Palanques, A., Rouiller, F., López-Jurado, J. L., Emelianov, M., Moutin, T. and Houpert, L.: Thick bottom nepheloid layers in the western Mediterranean generated by deep dense shelf water cascading, Prog. Oceanogr., 111, 1–23, https://doi.org/10.1016/j.pocean.2012.10.003, 2013.
- Puig, P.: Dense shelf water cascading and associated beforms, in: Atlas of Bedforms in the Western Mediterranean, edited by: Guillén, J., Acosta, J., Chiocci, F., and Palanques, A., Springer, Cham, https://doi.org/10.1007/978-3-319-33940-5_7, 2017.
- Puig, P., Company, J. B., Sardà, F., and Palanques, P.: Responses of deep-water shrimp populations to intermediate nepheloid layer detachments on the Northwestern Mediterranean continental margin, Deep Sea Res. I Oceanogr. Res. Pap., 48, 2195–2207, https://doi.org/10.1016/S0967-0637(01)00016-4, 2001.
- Puig, P., Palanques, A., Orange, D. L., Lastras, G., and Canals, M.: Dense shelf water cascades and sedimentary furrow formation in the Cap de Creus Canyon, northwestern Mediterranean Sea, Cont. Shelf Res., 28, 2017–2030, https://doi.org/10.1016/j.csr.2008.05.002, 2008.
- Puig, P., Palanques, A., and Martín, J.: Contemporary sediment-transport in submarine canyons, Annu. Rev. Mar. Sci., 6, 53–77, https://doi.org/10.1146/annurev-marine-010213-135037, 2014.
- Pusceddu, A., Mea, M., Canals, M., Heussner, S., Durrieu de Madron, X., Sanchez-Vidal, A., Bianchelli, S., Corinaldesi, C., Dell'Anno, A., Thomsen, L., and Danovaro, R.: Major consequences of an intense dense shelf water cascading event on deep-sea benthic trophic conditions and meiofaunal biodiversity,

- Biogeosciences, 10, 2659–2670, https://doi.org/10.5194/bg-10-2659-2013, 2013.
- Ribó, M., Puig, P., Palanques, A., and Lo Iacono, C.: Dense shelf water cascades in the Cap de Creus and Palamós submarine canyons during winters 2007 and 2008, Mar. Geol., 284, 175–188, https://doi.org/10.1016/j.margeo.2011.04.001, 2011.
- Rumín-Caparrós, A., Sanchez-Vidal, A., Calafat, A., Canals, M., Martín, J., Puig, P., and Pedrosa-Pàmies, R.: External forcings, oceanographic processes and particle flux dynamics in Cap de Creus submarine canyon, NW Mediterranean Sea, Biogeosciences, 10, 3493–3505, https://doi.org/10.5194/bg-10-3493-2013, 2013.
- Sadaoui, M., Ludwig, W., Bourrin, F., and Raimbault, P.: Controls, Budgets and Variability of Riverine Sediment Fluxes to the Gulf of Lions (NW Mediterranean Sea), J. Hydrol., 540, 1002–1015, https://doi.org/10.1016/j.jhydrol.2016.07.012, 2016.
- Sanchez-Vidal, A., Pasqual, C., Kerhervé, P., Heussner, S., Palanques, A., Durrieu de Madron, X., Canals, M., and Puig, P.: Impact of dense shelf water cascading on the transfer of organic matter to the deep western Mediterranean basin, Geophys. Res. Lett., 35, https://doi.org/10.1029/2007GL032825, 2008.
- Sanchez-Vidal, A., Calafat, A., Amblas, D., Cerdà-Domènech, M., and Fos, H.: CC1000 observatory data, SEANOE [data set], https://doi.org/10.17882/104746, 2025a.
- Sanchez-Vidal, A., Amblas, D., Arjona-Camas, M., Durrieu de Madron, X., Calafat, A., Cerdà-Domènech, M., Pena, L. D., and Espinosa, S.: CTD and ADCP data collected during the cruise FARDWO CC1, SEANOE [data set], https://doi.org/10.17882/105499, 2025b.
- Schlitzer, R.: Ocean Data View, https://odv.awi.de/ (last access: 25 August 2023), 2023.
- Schroeder, K., Josey, S. A., Herrmann, M., Grignon, L., Gasparini, G. P., and Bryden, H. L.: Abrupt warming and salting of the Western Mediterranean Deep Water: Atmospheric forcings and lateral advection, J. Geophys. Res., 115, C08029, https://doi.org/10.1029/2009JC005749, 2010.
- Schroeder, K., Ben Ismail, S., Bensi, M., Bosse, A., Chiggiato, K., Civitarese, G., Falcieri M, F., Fusco, G., Gacic, M., Gertman, I., Kubin, E., Malanotte-Rizzoli, P., Martellucci, R., Menna, M., Ozer, T., Taupier-Letage, I., Vargas-Yañez, M., Velaoras, D., and Vilibic, I.: A consensus-based, revised and comprehensive catalogue for Mediterranean water masses acronyms, Mediterranean Marine Science, 25, 783–791, https://doi.org/10.12681/mms.38736, 2024.
- Serrat, P., Ludwig, W., Navarro, B., and Blazi, J. L.: Variabilité spatio-temporelle des flux de matières en suspension d'un fleuve côtier méditerranéen: la Têt (France), Comptes Rendus de l'Académie des Sciences-Series IIA-Earth and Planetary Science, 333, 389–397, https://doi.org/10.1016/S1251-8050(01)01652-4, 2001.
- Smith, M. D., Knapp, A. K., and Collins, S. L.: A framework for assessing ecosystem dynamics in response to chronic resource alterations induced by global change, Ecology, 90, 3279–3289, https://doi.org/10.1890/08-1815.1, 2009.
- Somot, S., Sevault, F., and Déqué, M.: Transient climate change scenario simulation of the Mediterranean Sea for the twentyfirst century using a high-resolution ocean circulation model, Clim. Dynam., 27, 851–879, https://doi.org/10.1007/s00382-006-0167-z, 2006.

- Somot, S., Houpert, L., Sevault, F., Testor, P., Bosse, A., Taupier-Letage, I., Bouin, M. N., Waldman, R., Cassou, C., Sanchez-Gomez, E., Durrieu de Madron, X., Adloff, F., Nabat, P., and Herrmann, M.: Characterizing, modelling and understanding the climate variability of the deep water formation in the North-Western Mediterranean Sea, Clim. Dynam., 51, 1179–1210, https://doi.org/10.1007/s00382-016-3295-0, 2016.
- Taillandier, V., D'Ortenzio, F., Prieur, L., Conan, P., Coppola, L., Cornec, M., Dumas, F., Durrieu de Madron, X., Fach, B., Fourrier, M., Gentil, M., Hayes, D., and Husrevoglu, S.: Sources of the Levantine Intermediate Water in winter 2019, J. Geophys. Res. Oceans, 127, e2021JC017506, https://doi.org/10.1029/2021JC017506, 2022.
- Tesi, T., Puig, P., Palanques, A., and Goñi, M.: Lateral advection of organic matter in cascading-dominated submarine canyons, Prog. Oceanogr., 84, 185–203, https://doi.org/10.1016/j.pocean.2009.10.004, 2010.
- Testor, P., Bosse, A., Houpert, L., Margirier, F., Mortier, L., Le Goff, H., Dausse, D., Labaste, M., Kartensen, J., Hayes, D., Olita, A., Ribotti, A., Schroeder, K., Chiggiato, J., Onken, R., Heslop, E., Mourre, B., D'Ortenzio, F., Mayot, N., Lavigne, H., Durrieu de Madron, X., Bourrin, F., Many, G., Damien, P., Estournel, C., Marsaleix, P., Taupier-Letage, I., Raimbault, P., Waldman, R., Bouin, M. N., Giordani, H., Caniaux, G., Somot, S., Ducrocq, V., and Conan, P.: Multiscale observations of deep convection in the northwestern Mediterranean Sea during winter 2012–2013 using multiple platforms, J. Geophys. Res. Oceans, 123, 1745–1776, https://doi.org/10.1002/2016JC012671, 2018.
- Thurnherr, A. M.: A practical assessment of the errors associated with full-depth LADCP profiles obtained using Teledyne RDI Workhorse acoustic Doppler current profilers, J. Atmos. Ocean. Tech., 27, 1215–1227, https://doi.org/10.1175/2010JTECHO708.1, 2010.
- Thurnherr, A. M., Symonds, D., and Laurent, L. S.: Processing explorer ADCP data collected on slocum gliders using the LADCP shear method. In Proceedings of the 2015 IEEEOES 11th Current Waves and Turbulence Measurement CWTM, St. Petersburg, FL, USA 2–6 March 2015, https://doi.org/10.1109/CWTM.2015.7098134, 2015.

- Tubau, X., Lastras, G., Canals, M., Micallef, A., and Amblas, D.: Significance of the drainage pattern for submarine canyon evolution: The Foix Canyon System, Northwestern Mediterranean Sea, Geomorphology, 184, 20–37, https://doi.org/10.1016/j.geomorph.2012.11.007, 2013.
- Ulses, C., Estournel, C., Bonnin, J., Durrieu de Madron, X., and Marsaleix, P.: Impact of storms and dense water cascading on shelf-slope exchanges in the Gulf of Lion (NW Mediterranean), J. Geophys. Res. Oceans, 113, https://doi.org/10.1029/2006JC003795, 2008a.
- Ulses, C., Estournel, C., Puig, P., Durrieu de Madron, X., and Marsaleix, P.: Dense shelf water cascading in the northwestern Mediterranean during the cold winter 2005: Quantification of the export through the Gulf of Lion and the Catalan margin, Geophys. Res. Lett., 35, https://doi.org/10.1029/2008GL033257, 2008b.
- Visbeck, M.: Deep velocity profiling using lowered acoustic Doppler current profilers: Bottom track and inverse solutions, J. Atmos. Ocean. Tech. 19, 794–807, https://doi.org/10.1175/1520-0426(2002)019<0794:DVPULA>2.0.CO;2, 2002.
- Walsh, J. P. and Nittrouer, C. A.: Understanding fine-grained river-sediment dispersal on continental margins, Mar. Geol., 263, 34–45, https://doi.org/10.1016/j.margeo.2009.03.016, 2009.
- Wilson, G. W. and Hay, A. E.: Acoustic backscatter inversion for suspended sediment concentration and size: a new approach using statistical inverse theory, Cont. Shelf Res., 106, 130–139, https://doi.org/10.1016/j.csr.2015.07.005, 2015.
- Zúñiga, D., Flexas, M. M., Sanchez-Vidal, A., Coenjaerts, J., Calafat, A., Jordà, G., García-Orellana, J., Puigdefàbregas, J., Canals, M., Espino, M., Sardà, M., and Company, J. B.: Particle fluxes dynamics in Blanes submarine canyon (Northwestern Mediterranean), Prog. Oceanogr., 82, 239–251, https://doi.org/10.1016/j.pocean.2009.07.002, 2009.